

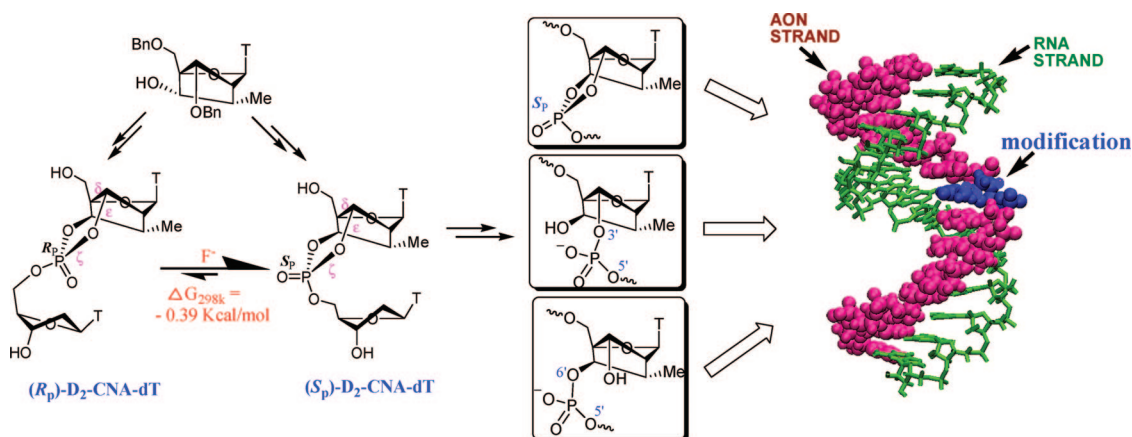
Double Sugar and Phosphate Backbone-Constrained Nucleotides: Synthesis, Structure, Stability, and Their Incorporation into Oligodeoxynucleotides

Chuanzheng Zhou, Oleksandr Plashkevych, and Jyoti Chattopadhyaya*

Department of Bioorganic Chemistry, Box 581, ICM, Biomedical Center,
Uppsala University, SE-751 23 Uppsala, Sweden

jyoti@boc.uu.se

Received August 12, 2008



Two diastereomerically pure carba-LNA dioxaphosphorinane nucleotides [(S_p)- or (R_p)-D₂-CNA], simultaneously conformationally locked at the sugar and the phosphate backbone, have been designed and synthesized. Structural studies by NMR as well as by ab initio calculations showed that in (S_p)- and (R_p)-D₂-CNA the following occur: (i) the sugar is locked in extreme North-type conformation with $P = 11^\circ$ and $\Phi_m = 54^\circ$; (ii) the six-membered 1,3,2-dioxaphosphorinane ring adopts a half-chair conformation; (iii) the fixed phosphate backbone δ , ϵ , and ζ torsions were found to be δ [*gauche*(+)], ϵ [*cis*], ζ [*antiperiplanar*(+)] for (S_p)-D₂-CNA, and δ [*gauche*(+)], ϵ [*cis*], ζ [*antiperiplanar*(-)] for (R_p)-D₂-CNA. It has been found that F⁻ ion can catalyze the isomerization of pure (S_p)-D₂-CNA or (R_p)-D₂-CNA to give an equilibrium mixture ($K = 1.94$). It turned out that at equilibrium concentration the (S_p)-D₂-CNA isomer is preferred over the (R_p)-D₂-CNA isomer by 0.39 kcal/mol. The chemical reactivity of the six-membered dioxaphosphorinane ring in D₂-CNA was found to be dependent on the internucleotidic phosphate stereochemistry. Thus, both (S_p)- and (R_p)-D₂-CNA dimers (**17a** and **17b**) were very labile toward nucleophile attack in concentrated aqueous ammonia [$t_{1/2} = 12$ and 6 min, respectively] to give carba-LNA-6',5'-phosphodiester (**21**) ≈ 70 –90%, carba-LNA-3',5'-phosphodiester (**22**) $\approx 10\%$, and carba-LNA-6',3'-phosphodiester (**23**) $< 10\%$. In contrast, the (S_p)-D₂-CNA was about 2 times more stable than (R_p)-D₂-CNA under hydrazine hydrate/pyridine/AcOH (pH = 5.6) [$t_{1/2} = 178$ and 99 h, respectively], which was exploited in the deprotection of pure (S_p)-D₂-CNA-incorporated antisense oligodeoxynucleotides (AON). Thus, after removal of the solid supports from the (S_p)-D₂-CNA-modified AONs by BDU/MeCN, they were treated with hydrazine hydrate in pyridine/AcOH to give pure AONs in 35–40% yield, which was unequivocally characterized by MALDI-TOF to show that they have an intact six-membered dioxaphosphorinane ring. The effect of pure (S_p)-D₂-CNA modification in the AONs was estimated by complexing to the complementary RNA and DNA strands by the thermal denaturation studies. This showed that this cyclic phosphotriester modification destabilizes the AON/DNA and AON/RNA duplex by about -6 to -9 °C/modification. Treatment of (S_p)-D₂-CNA-modified AON with concentrated aqueous ammonia gave carba-LNA-6',5'-phosphodiester modified AON ($\sim 80\%$) plus a small amount of carba-LNA-3',5'-phosphodiester-modified AON ($\sim 20\%$). It is noteworthy that Carba-LNA-3',5'-phosphodiester modification stabilized the AON/RNA duplex by $+4$ °C/modification (*J. Org. Chem.* **2009**, *74*, 118), whereas carba-LNA-6',5'-phosphodiester modification destabilizes both AON/RNA and AON/DNA significantly (by -10 to -19 °C/modification), which, as shown in our comparative CD studies, that the cyclic phosphotriester modified AONs as well as carba-LNA-6',5'-phosphodiester modified AONs are much more weakly stacked than carba-LNA-3',5'-phosphodiester-modified AONs.

Introduction

The conformationally constrained oligonucleotides^{1,2} have been found to play an important role in the study of structure

and activity of nucleic acids. They also have been found to be important in the antisense and RNAi application^{3–5} owing to the fact that when they are introduced into the antisense oligonucleotides (AON), the modified AON binds to the target

(1) Leumann, C. J. *Bioorg. Med. Chem.* **2002**, *10*, 841–854.

(2) Mathe, C.; Perigaud, C. *Eur. J. Org. Chem.* **2008**, 1489–1505.

RNA strongly because of reduced entropy penalty, without, however, compromising the enzymatic properties.

The conformation of nucleotide is determined by phosphate backbone torsion angles as well as by the endocyclic sugar torsions and the orientation of the base relative to the sugar (Figure 1A).⁶ Conformationally constrained nucleosides and nucleotides can be obtained by constraining any one or several of these torsion angles. The known conformationally constrained nucleosides and nucleotides^{2,7} can be classified into three types. The first type is constrained in the pentose–sugar moiety. LNA^{8,9} (Figure 1B), ENA¹⁰ (Figure 1C), and their analogues^{11–15} are the major representatives of this class, in which the sugar puckering (torsion angles ν_0 – ν_4) are fixed by the sugar modification. Constraining torsion angle χ composes the second type of conformationally constrained nucleosides and nucleotides. Generally, the torsion angle χ is fixed by linking the base with phosphate (Figure 1D)^{16–18} or sugar (Figure 1E)¹⁹ by an alkyl arm, and as a result, not only the χ but also the sugar puckering or/and backbone torsion angles are constrained. The third type is constrained in the phosphate backbone moiety by linking the nonbridging phosphate oxygen through an alkyl chain to sugar carbons by formation of cyclic phosphate rings on the phosphate backbone. This type of conformationally constrained nucleosides and nucleotides include unsaturated 7-membered C5', P-cyclic phosphotriester^{20,21} (Figure 1F), α,β -D-CNA^{22,23} (Figure 1G), α,β,γ -D-CNA²⁴ (Figure 1H), ε,ζ -D-CNA in *xylo* configuration²⁵ (Figure 1I), δ,ε,ζ -D-CNA²⁴ (Figure 1J), ν_2,ε,ζ -D-CNA²⁶ (Figure 1K), and ε,ζ -constrained nucleotides^{27,28} (Figure 1L).

It should be noted that in δ,ε,ζ -D-CNA²⁴ (Figure 1J), ν_2,ε,ζ -D-CNA²⁶ (Figure 1K), and ε,ζ -constrained nucleotides^{27,28} (Figure 1L), constraining backbone torsions ε and ζ also leads to locking the sugar puckering in the South conformation. Dimerization of a North-type conformationally constrained LNA thymidine with the α,β -D-CNA into LNA/ α,β -D-CNA (Figure 1M) has also been reported recently.²⁹ However, the fusion of a conformationally constrained North-type sugar-containing nucleotide with the conformationally constrained D-CNA-type cyclic phosphate modification to synthesize the hyperconstrained system has not been reported to date. We achieved such a molecular construction of double-constrained nucleotide (general formula: D₂-CNA, Figure 1N) in the present work by tightening the flexibility of the sugar–phosphate backbone by introducing (1) a 2',4'-ethylene bridge on the pentose sugar moiety as well as by (2) the introduction of a cyclic 1,3,2-dioxaphosphorinane rings on the internucleotidic phosphate linkage. Here, we report synthesis and structure/conformational analysis of the diastereoisomers of D₂-CNA. The chemical and enzymatic stability of these cyclic 1,3,2-dioxaphosphorinane rings on the internucleotidic phosphate linkage have also been studied. This has also led us to understand how different types of the sugar–phosphate backbones dictate the thermal stability of the homo and heteroduplexes as a result of cooperative stacking or its distortions in the modified AON strand compared to the native counterpart.

Results and Discussion

1.0. Synthesis of Diastereomerically Pure (*S_p*)-D₂-CNA-dT (17a) and (*R_p*)-D₂-CNA-dT dimers (17b). Recently, we have reported a novel synthetic strategy for the synthesis of five- and six-membered conformationally constrained 2',4'-carbocyclic thymidines (carba-LNA-T, Figure 1B and carba-ENA-T, Figure 1C) using an intramolecular free-radical ring-closure reaction.^{13,14} The sugar moieties of the carba-LNA and carba-ENA have been shown¹³ to be locked into North-type conformation ($P = 15^\circ$ and 19° , respectively). Subsequently, during our effort to functionalize the carbocyclic moiety of carba-LNA, we obtained a key derivative, 6'(*S*)-OH carba-LNA **1**³⁰ (Scheme 1). Analysis of the conformation of carba-LNA **1** suggested that it is a structurally suitable scaffold to give a 1,3,2-dioxaphosphorinane ring with the 5'-*O*-phosphate of an appropriately protected second nucleotide to give cyclic 1,3,2-dioxaphosphorinane containing D₂-CNA-dT dimers.

1.1. Intramolecular Displacement Reaction: Strategy I. Thus, from starting material **1**, we designed a route (Scheme 1) to synthesize double-constrained D₂-CNA-dT dimer. Compound **1** was first transformed to the O6'-tosylated product **2** in high yield (94%) by reaction with 4-tosyl chloride in pyridine. Compound **2** was debenzylated using 20% Pd(OH)₂/C and ammonium formate under reflux in methanol for 7 h and then 5'-dimethoxytritylated to give **4** (two steps: 74%), which was coupled with thymidine-5'-phosphoramidite **5** in dry MeCN using 5-ethylthio-1*H*-tetrazole as a catalyst and then oxidized with I₂/THF–H₂O–pyridine to give a 1:1 mixture of two diastereomers of **6**. D₂-CNA-dT **7** was expected²⁴ to be obtained

- (3) Herdewijn, P. *Biochim. Biophys. Acta* **1997**, *1489*, 167–179.
- (4) Kaur, H.; Babu, R.; Maiti, S. *Chem. Rev.* **2007**, *107*, 4672–4697.
- (5) Bumcrot, D.; Manoharan, M.; Kotliansky, V.; Sah, D. W. Y. *Nature Chem. Bio.* **2006**, *2*, 711–719.
- (6) Saenger, W. *Principles of Nucleic Acid Structure*; Springer-Verlag: New York, 1983.
- (7) Herdewijn, P. *Biochim. Biophys. Acta* **1999**, *1489*, 167–179.
- (8) Singh, S. K.; Nielsen, P.; Koshkin, A. A.; Wengel, J. *Chem. Commun.* **1998**, 455–456.
- (9) Obika, S.; Morio, K.; Nanbu, D.; Imanishi, T. *Chem. Commun.* **1997**, 1643–1644.
- (10) Morita, K.; Takagi, M.; Hasegawa, C.; Kaneko, M.; Tsutsumi, S.; Sone, J.; Ishikawa, T.; Imanishi, T.; Koizumi, M. *Bioorg. Med. Chem.* **2003**, *11*, 2211–2226.
- (11) Varghese, O.; Barman, J.; Pathmasiri, W.; Plashkevych, O.; Honcharenko, D.; Chattopadhyaya, J. *J. Am. Chem. Soc.* **2006**, *128*, 15173–15187.
- (12) Singh, S. K.; Kumar, R.; Wengel, J. *J. Org. Chem.* **1998**, *63*, 10035–10039.
- (13) Srivastava, P.; Barman, J.; Pathmasiri, W.; Plashkevych, O.; Wenska, M.; Chattopadhyaya, J. *J. Am. Chem. Soc.* **2007**, *129*, 8362–8379.
- (14) Zhou, C.; Plashkevych, O.; Chattopadhyaya, J. *Org. Biomol. Chem.* **2008**, *6*, 4627–4633.
- (15) Albak, N.; Petersen, M.; Nielsen, P. *J. Org. Chem.* **2006**, *71*, 7731–7740.
- (16) Børsting, P.; Nielsen, P. *Chem. Commun.* **2002**, 2140–2141.
- (17) Seio, K.; Wada, T.; Sakamoto, K.; Yokoyama, S.; Sekine, M. *J. Org. Chem.* **1996**, *61*, 1500–1504.
- (18) Sekine, M.; Kurasawa, O.; Shohda, K.; Seio, K.; Wada, T. *J. Org. Chem.* **2000**, *65*, 3571–3578.
- (19) Bevierre, M. O.; Mesmaeker, A. D.; Wolf, R. M.; Freier, S. M. *Bioorg. Med. Chem. Lett.* **1994**, *4*, 237–240.
- (20) Sørensen, A. M.; Nielsen, P. *Org. Lett.* **2000**, *2*, 4217–4219.
- (21) Sørensen, A. M.; Nielsen, K. E.; Vogg, B.; Jacobsen, J. P.; Nielsen, P. *Tetrahedron* **2001**, *57*, 10191–10201.
- (22) Le Clézio, I.; Escudier, J. M.; Vigroux, A. *Org. Lett.* **2003**, *5*, 161–164.
- (23) Dupouy, C.; Le Clézio, I.; Lavedan, P.; Gornitzka, H.; Escudier, J. M.; Vigroux, A. *Eur. J. Org. Chem.* **2006**, 5515–5525.
- (24) Le Clézio, I.; Gornitzka, H.; Escudier, J. M.; Vigroux, A. *J. Org. Chem.* **2005**, *70*, 1620–1629.
- (25) Dupouy, C.; Lavedan, P.; Escudier, J. M. *Tetrahedron* **2007**, *63*, 11235–11243.
- (26) Dupouy, C.; Lavedan, P.; Escudier, J. M. *Eur. J. Org. Chem.* **2008**, 1285–1294.
- (27) Børsting, P.; Nielsen, K. E.; Nielsen, P. *Org. Biomol. Chem.* **2005**, *3*, 2183–2190.

(28) Børsting, P.; Christensen, M. S.; Steffansen, S. I.; Nielsen, P. *Tetrahedron* **2006**, *62*, 1139–1149.

(29) Dupouy, C.; Lavedan, P.; Escudier, J. M. *Eur. J. Org. Chem.* **2007**, 5256–5264.

(30) Zhou, C.; Liu, Y.; Andaloussi, M.; Badgujar, N.; Plashkevych, O.; Chattopadhyaya, J. *J. Org. Chem.* **2009**, *74*, 118–134.

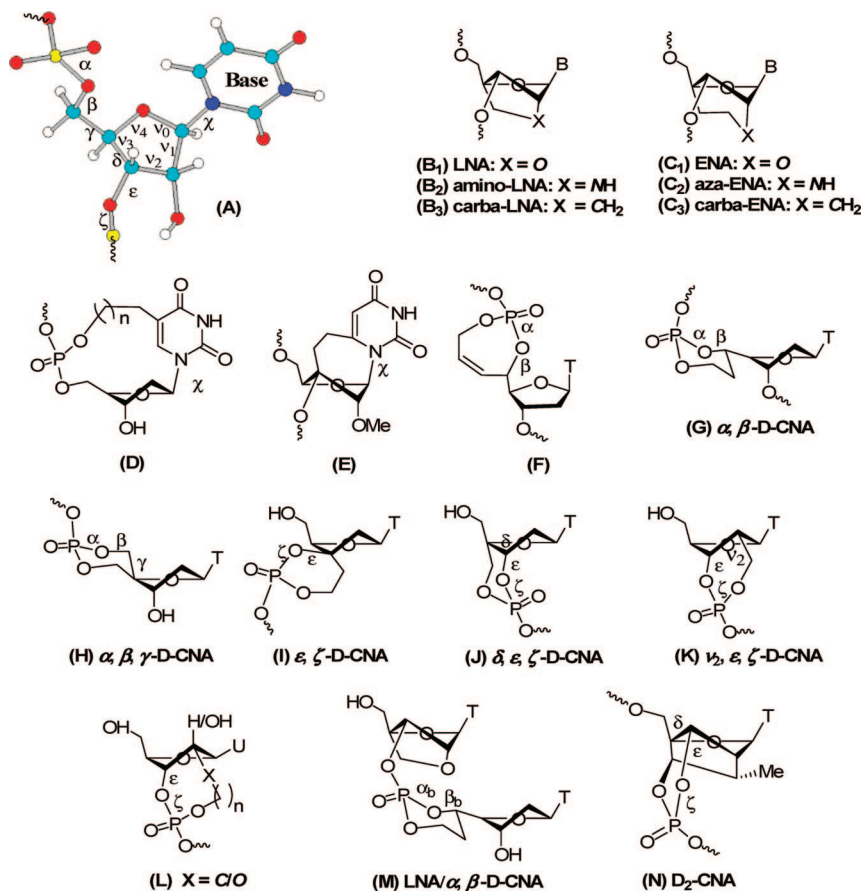
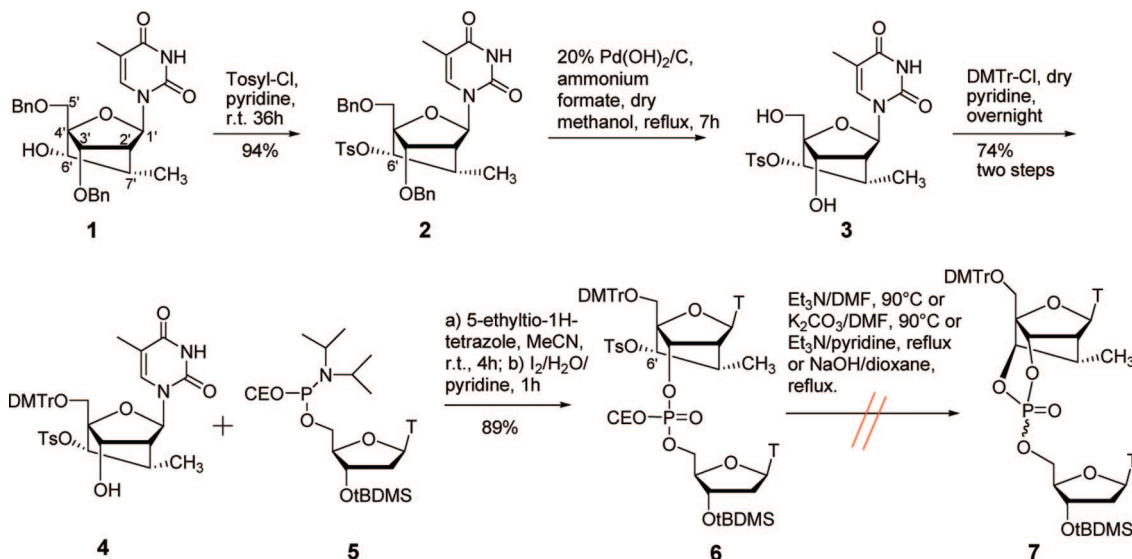


FIGURE 1. (A) Definition of torsion angles for a nucleotide unit. (B–N) Formulas represent structures of different types of conformational-constrained nucleotides (refs 8–29).

SCHEME 1



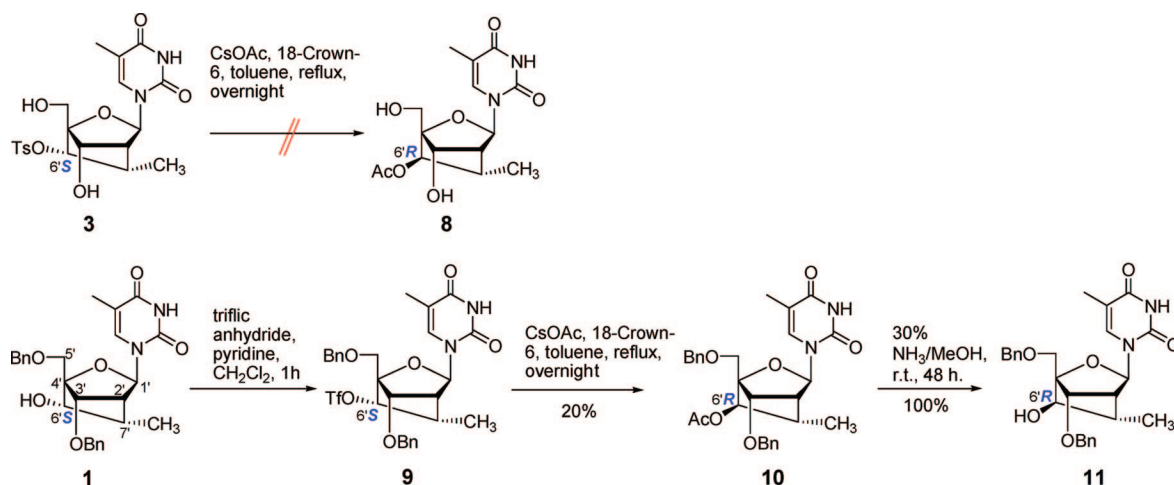
by base-induced cyclization of the acyclic precursor **6**, but that was not found to be the case, although several different conditions were tried, including (a) Et₃N/DMF, 90 °C, (b) K₂CO₃/DMF, 90 °C, (c) Et₃N/pyridine, reflux, or (d) NaOH/dioxane, reflux. We speculate that the rigidity of the carbocyclic moiety of carba-LNA precludes the possibility that C6'-OTs in **6** can alter its conformation to form an in-line transition state with the P=O nucleophile, which is required for the S_N2 substitution to take place.

1.2. One-Step Ring-Closure by Phosphitylation of the Bis-Hydroxy Intermediate: Strategy II. An alternative approach to form 1,3,2-dioxaphosphorinane ring is coupling of a *cis*-diol with phosphoramidite followed by oxidation.^{31,32} In carba-LNA **1**, the 3'-OH and 6'-OH can serve as a vicinal diol

(31) Pavey, J. B. J.; Cosstick, R.; O'Neil, I. A. *Tetrahedron Lett.* **1998**, *39*, 8923–8924.

(32) Riley, A. M.; Guedat, P.; Schlewer, G.; Spiess, B.; Potter, B. V. *J. Org. Chem.* **1998**, *63*, 295–305.

SCHEME 2



system, but these two hydroxyls are stereochemically *trans* to each other and cannot give easily a six-membered cyclic phosphate with phosphoradiazidite in view of the strain of the resulting trans-fused system. We argued that the inversion of the configuration of 6'-OH will result in the 6'-OH and 3'-OH pointing in the same direction, cisoid to each other, and thereby formation of a cyclic 1,3,2-dioxaphosphorinane ring will be favorable. Reaction of tosylated alcohol **3** with cesium acetate and 18-crown-6 is an effective method for the inversion of configuration of secondary alcohols.^{33,34} Hence, compound **3** was treated with cesium acetate and 18-crown-6 in toluene under reflux, which, however, did not give the expected product **8** (Scheme 2). Given the fact that 6'-tosylate was not a very good leaving group, carba-LNA **1** was transformed to 6'-*O*-triflate **9** which is known to be 10⁵ times more reactive than that of the 6'-tosylate.³⁵ Thus, compound **9** with C6'-*S* configuration could be transformed to **10** with C6'-*R* configuration by the action of cesium acetate and 18-crown-6 in toluene under reflux, albeit with a very poor yield (20%). Deacetylation of compound **10** was performed using 30% NH₃/MeOH at rt for 2 days to give **11** quantitatively.

Alternatively, compound **11** (C6'-*R*) could be obtained in satisfactory yield by oxidizing **1** (C6'-*S*) to the corresponding ketone **12** with Dess–Martin periodinane, followed by reduction with NaBH₄ (Scheme 3). These successive oxidation–reduction steps gave 54% of **11** (C6'-*R*) as well as 40% of recovered substrate **1** (C6'-*S*), which could be recycled to give more of product **11**. Compound **11** was debenzylated using 20% Pd(OH)₂/C and ammonium formate under reflux in methanol for 3 h and then subjected to 5'-dimethoxytritylation to give **13** (two steps: 77%). Compound **13** was coupled with freshly prepared thymidine-5'-phosphoradiazidite **14** in dry MeCN using 5-ethylthio-1*H*-tetrazole as a catalyst and then converted with I₂/THF–H₂O–pyridine to give two pure *P*-diastereomers, protected (by both 5'-*O*-DMTr and 3'-*b*-*O*-tBDMS) pure (S_p)-D₂-CNA-dT dimer **15a** in 39% yield and pure (R_p)-D₂-CNA-dT **15b** in 16% yield.

1.3. NMR Characterization of Protected (by Both 5'-*O*-DMTr and 3'-*b*-*O*-tBDMS) Pure (S_p)-D₂-CNA-dT Dimer **15a and (R_p)-D₂-CNA-dT **15b**.** ¹H, ¹H {³¹P}, and ¹³C NMR experiments have been used to witness the formation of

six-membered cyclic 1,3,2-dioxaphosphorinane ring in compounds **15a** and **15b**. As shown in Figure S50 (Supporting Information), comparing the ¹H with ¹H {³¹P} NMR spectra of compound **15a** as well as **15b**, we have found that both H3'_a and H6'_a are coupled with the ³¹P of the internucleotide phosphate, giving the coupling constants of ³J_{p,H3'a} ≈ 16–18.0 Hz and ³J_{p,H6'a} ≈ 24 Hz. The two-bond couplings between the internucleotide-³¹P and C3'_a and C6'_a have also been observed, and thus, in the ¹³C NMR spectra, the resonances of C3'_a and C6'_a are doublets with ²J_{p,C3'a} = 8.8 Hz, ²J_{p,C6'a} = 6.6 Hz for compound **15a** (Figure S28, Supporting Information) and ²J_{p,C3'a} = 10.1 Hz and ²J_{p,C6'a} = 5.5 Hz for compound **15b** (Figure S40, Supporting Information). The exocyclic substitution on phosphorus in **15a** is orientated axially, resulting in an S_p configuration of the phosphorus chiral center, while in **15b** it is in an R_p configuration. These configuration assignments of **15a** and **15b** have been confirmed in two different ways: First, the chemical shift of phosphorus (δ ³¹P) for compound **15a** (δ_{31p} = –8.06 ppm, Figure S25, Supporting Information) and **15b** (δ_{31p} = –7.06 ppm) fall in the typical range of the six-membered cyclic phosphate esters.³⁶ Furthermore, δ 31p of **15a** has an upfield shift compared to that of **15b**, which is consistent with the well-established empirical rule in that the axially substituted diastereomer has an upfield ³¹P chemical shift.³⁷ Second, a medium-strong correlation (ca. 3–4 Å) between H7'_a and H5'_b has been observed in the NOESY spectrum of compound **15a** (Figure S35, Supporting Information), while for **15b** this cross peak does not exist.

1.4. Removal of 3'-*b*-*O*-tBDMS group and 5'-*O*-DMTr Groups from Pure (S_p)-D₂-CNA-dT Dimer **15a and (R_p)-D₂-CNA-dT **15b**.** Pure **15a** was treated with 1 M TBAF/THF for 20 min to deprotect the 3'-*b*-*O*-tBDMS group, but unexpectedly, two *P*-diastereomers **16a** and **16b** were obtained in a ratio of 84/16 (NMR) as a mixture (see below, section 5.0 for the isomerization study), which were separated by silica gel chromatography to give two pure diastereomers, 5'-*O*-DMTr protected (S_p)-D₂-CNA-dT dimer **16a** (75%) and (R_p)-D₂-CNA-dT **16b** (14%). Similarly, treatment of pure **15b** with 1M TBAF/THF for 20 min gave the same pure products **16a** (32%) and pure **16b** (58%). It turned out that the internucleotide phosphotriester group in the major (S_p)-D₂-CNA-dT dimer **16a**

(33) Torisawa, Y.; Okabe, H.; Ikegami, S. *Chem. Lett.* **1984**, 1555–1556.

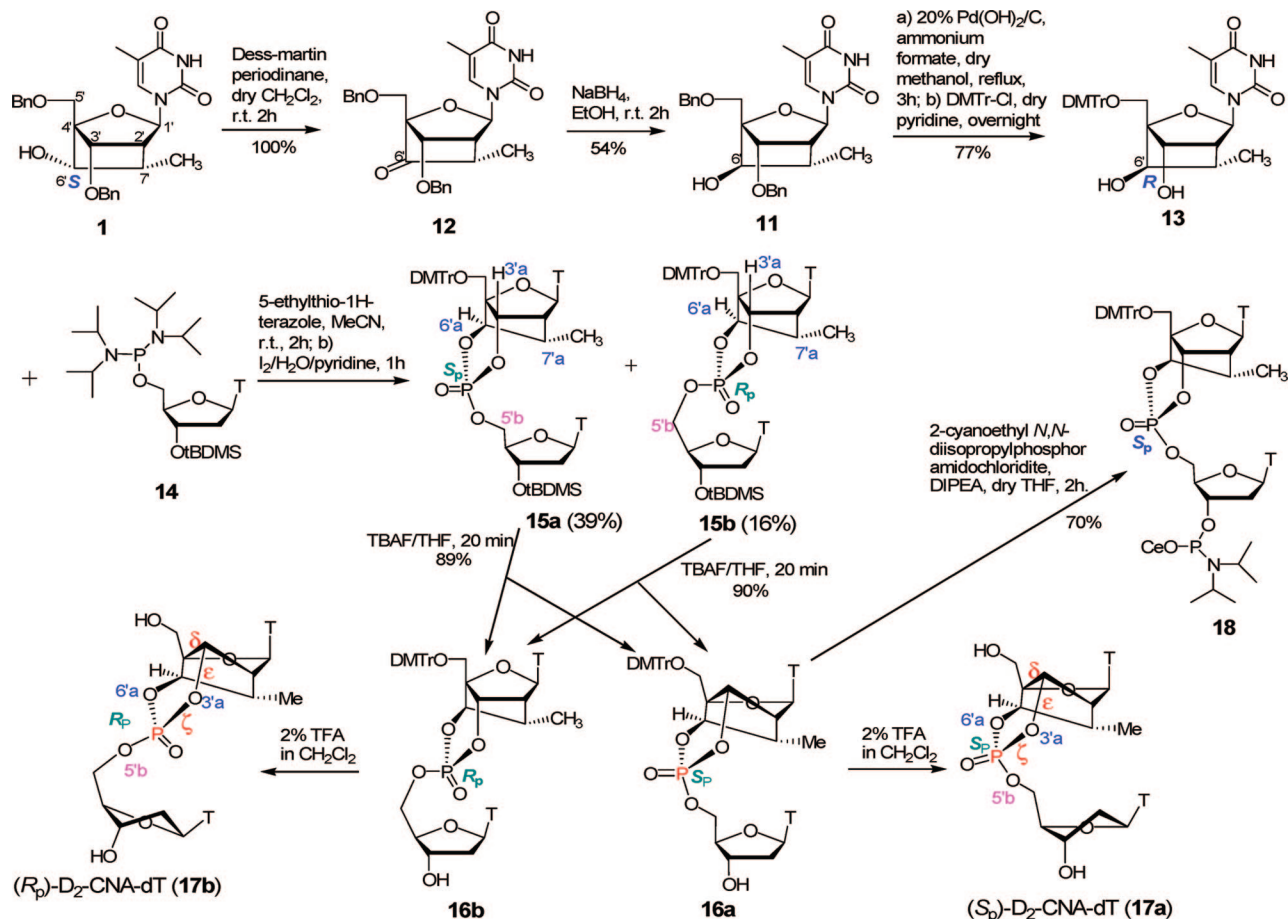
(34) Sato, K.; Yoshitomo, A. *Chem. Lett.* **1995**, 39–40.

(35) Stang, P.; Hanack, M.; Subramanian, L. R. *Synthesis* **1982**, 85–126.

(36) Gorenstein, D. G. *J. Am. Chem. Soc.* **1975**, 97, 898–900.

(37) Gorenstein, D. G.; Rowell, R. *J. Am. Chem. Soc.* **1979**, 101, 4925–4928.

SCHEME 3



was more stable under the deprotection conditions (see section 3.0) than the (R_p) counterpart; hence, the former was incorporated in to the substituted oligonucleotides (see section 6.0).

Compound **16a** or **16b** was treated with 2% TFA/ CH_2Cl_2 for 10 min to give fully deprotected (S_p)- D_2 -CNA-dT dimer **17a** or (R_p)- D_2 -CNA-dT dimer **17b** quantitatively, which was used for structure and stability study.

2.0. Study of Molecular Structures of (S_p)- D_2 -CNA-dT Dimer **17a and (R_p)- D_2 -CNA-dT Dimer **17b** Based on NMR and Ab Initio Calculations.** For (S_p)- D_2 -CNA-dT dimer **17a** and (R_p)- D_2 -CNA-dT dimer **17b**, the experimental vicinal coupling constants ($^3J_{\text{H,H}}$, $^3J_{\text{P,H}}$, and $^3J_{\text{P,C}}$) have been obtained from homo- and heterodecoupling experiments (see Figures S80 and S90, Supporting Information) and are listed in Table 1. These coupling constants have been compared with the theoretical coupling constants obtained by back calculations from the corresponding ab initio calculated torsion angles employing the Haasnoot–de Leeuw–Altona generalized Karplus equation.^{38,39} The geometry optimizations of the D_2 -CNA-dT dimers **17a** and **17b** have been carried out at the Hartree–Fock level using the 6-31G** basis set as implemented in the GAUSSIAN 98 program package⁴⁰ to give the theoretical torsion angles.

As shown in Table 1, the experimental vicinal coupling constants of the 5'-end D_2 -CNA in both dimers (S_p)-**17a** and (R_p)-**17b** are well reproduced by applying the Haasnoot–de Leeuw–Altona generalized Karplus equation^{38,39} to the torsions

obtained from the ab initio calculations. This indicates that the modified D_2 -CNA moiety located at the 5'-end of the dimers **17a** and **17b** are indeed in a rigid locked conformation, and their average molecular structures observed experimentally are close to that of the minimized theoretical structure. The conformational analysis of the D_2 -CNA in both dimers **17a** and **17b** reveals that the furanose rings are locked in the typical North conformation with phase angle $P = 11^\circ$ and puckering amplitude $\Phi_m = 54^\circ$. The formation of six-membered 1,3,2-dioxaphosphorinane ring by linking the 3'-O and 6'-O in D_2 -CNA results in more tightly constrained North conformation for the furanose ring, given that $P = 18^\circ$ in compound **11**³⁰ (Table S1, Supporting Information) and $P = 19^\circ$ in LNA and ENA.⁴¹

In dimers **17a** and **17b**, the $^3J_{\text{P,H}3'a}$ have been found to be 16–17 Hz, which corresponds to ca. 145° for the $\Phi_{\text{P-O}3'-\text{C}3'-\text{H}3'a}$. The large coupling constants of $^3J_{\text{P,H}6'a}$ (~ 25 Hz) suggested $\Phi_{\text{P-O}3'-\text{C}3'-\text{H}6'a}$ are nearly 180° . Thus, the six-membered 1,3,2-dioxaphosphorinane in D_2 -CNA adopts a half-chair conforma-

(38) Haasnoot, C. A. G.; de Leeuw, F. A. A. M.; Altona, C. *Tetrahedron* **1980**, *36*, 2783–2792.

(39) Altona, C.; Sundaralingam, M. *J. Am. Chem. Soc.* **1972**, *94*, 8205–1822.

(40) Frisch, M. J.; Trucks, G. W.; Schlegel, H. B.; Scuseria, G. E.; Robb, M. A.; Cheeseman, J. R.; Zakrzewski, V. G.; Montgomery, J. J. A.; Stratmann, R. E.; Burant, J. C.; Dapprich, S.; Millam, J. M.; Daniels, A. D.; Kudin, K. N.; Strain, M. C.; Farkas, O.; Tomasi, J.; Barone, V.; Cossi, M.; Cammi, R.; Mennucci, B.; Pomelli, C.; Adamo, C.; Clifford, S.; Ochterski, J.; Petersson, G.; Ayala, P. Y.; Cui, Q.; Morokuma, K.; Malick, D. K.; Rabuck, A. D.; Raghavachari, K.; Foresman, J. B.; Cioslowski, J.; Ortiz, J. V.; Baboul, A. G.; Stefanov, B. B.; Liu, G.; Liashenko, A.; Piskorz, P.; Komaromi, I.; Gomperts, R.; Martin, R. L.; Fox, D. J.; Keith, T.; Al-Laham, M. A.; Peng, C. Y.; Nanayakkara, A.; Gonzalez, C.; Challacombe, M.; Gill, P. M. W.; Johnson, B. G.; Chen, W.; Wong, M. W.; Andres, J. L.; Head-Gordon, M.; S., R. E.; Pople, J. A. *Gaussian 98 (Revision A.6)*; Gaussian, Inc: Pittsburgh PA, 1998.

TABLE 1. Experimental and Calculated Vicinal $^3J_{\text{H,H}}$, $^3J_{\text{P,H}}$, and $^3J_{\text{P,C}}$ Coupling Constants and Torsion Angles in (S_{p})-D₂-CNA-dT Dimer **17a** and (R_{p})-D₂-CNA-dT Dimer **17b**

| | torsion ($\Phi_{\text{H,H}}$) | (S_{p})-D ₂ -CNA-dT dimer 17a | | | | (R_{p})-D ₂ -CNA-dT dimer 17b | | | | |
|---|---|--|------------------------------|------------------------------|-----------------------|--|------------------------------|------------------------------|-----------------------|-----|
| | | $\Phi_{\text{H,H}}$, ab initio ^a | $J_{\text{H,H}}$, cal Hz | $J_{\text{H,H}}$, exp Hz | $ \Delta^3J $, Hz | $\Phi_{\text{H,H}}$, ab initio ^a | $J_{\text{H,H}}$, cal Hz | $J_{\text{H,H}}$, exp Hz | $ \Delta^3J $, Hz | |
| 5'-end | $^3J_{\text{H-1}^{\text{a}},\text{H-2}^{\text{a}}}$ | H1'-C1'-C2'-H2' | 76.2 | 0.9 | 0.0 | 0.9 | 76.5 | 0.9 | 0.7 | 0.2 |
| | $^3J_{\text{H-2}^{\text{a}},\text{H-3}^{\text{a}}}$ | H2'-C2'-C3'-H3' | 57.3 | 4.1 | 2.6 | 1.5 | 57.7 | 4.0 | 1.6 | 2.4 |
| | $^3J_{\text{H-2}^{\text{a}},\text{H-7}^{\text{a}}}$ | H2'-C2'-C7'-H7' | 46.2 | 5.7 | 5.0 | 0.7 | 45.6 | 5.8 | 4.9 | 0.9 |
| | $^3J_{\text{H-7}^{\text{a}},\text{H-8}^{\text{a}}}$ | H7'-C7'-C8'-H8' | -70.4, 168.5, 49.0 | 6.7 ^b | 7.4 | 0.7 | -70.1, 168.7, 49.1 | 6.6 ^b | 7.3 | 0.7 |
| | $^3J_{\text{H-6}^{\text{a}},\text{H-7}^{\text{a}}}$ | H6'-C6'-C7'-H7' | 57.3 | 2.0 | 0 | 2.0 | -116.5 | 2.0 | 0 | 2.0 |
| | $^3J_{\text{P,H-3}^{\text{a}}}$ | P-O3'-C3'-H3' | 135.1 | 13.6 | 17.0 | 3.4 | 143.9 | 16.5 | 16.1 | 0.4 |
| | $^3J_{\text{P,H-6}^{\text{a}}}$ | P-O-C3'-H6' | -172.2 | 22.7 | 24.9 | 2.2 | 178.9 | 23.0 | 25.2 | 2.2 |
| | $^2J_{\text{P,C-3}^{\text{a}}}$ | | | | 8.3 | | | | 9.4 | |
| | $^2J_{\text{P,C-6}^{\text{a}}}$ | | | | 6.9 | | | | 6.1 | |
| | $^3J_{\text{P,C-2}^{\text{a}}}$ | P-O3'-C3'-C2' | -96.9 | 1.2 | 0 | 1.2 | -88.2 | 0.8 | 0 | 0.8 |
| | $^3J_{\text{P,C-4}^{\text{a}}}$ | P-O3'-C3'-C4' | 7.5 | 7.9 | 6.9 | | 16.4 | 7.4 | 6.9 | |
| | $^3J_{\text{P,C-4}^{\text{a}}}$ | P-O-C6'-C4' | -50.4 | 3.3 | | | -59.2 | 2.2 | | |
| | $^3J_{\text{P,C-7}^{\text{a}}}$ | P-O-C6'-C7' | 62.8 | 1.8 | 0 | 1.8 | 53.7 | 2.9 | 0 | 2.9 |
| | 3'-end | $^3J_{\text{H-1}^{\text{b}},\text{H-2}^{\text{b}}}$ | H1'-C1'-C2'-H2' | 161.0 | 10.2 | 6.4 | 160.0 | 10.1 | 6.7 | |
| $^3J_{\text{H-1}^{\text{b}},\text{H-2}^{\text{b}}}$ | | H1'-C1'-C2'-H2'' | 39.2 | 5.2 | 7.0 | 38.8 | 5.2 | 6.4 | | |
| $^3J_{\text{H-2}^{\text{b}},\text{H-3}^{\text{b}}}$ | | H2'-C2'-C3'-H3' | -36.0 | 5.9 | 4.0 | -38.8 | 5.4 | 4.9 | | |
| $^3J_{\text{H-2}^{\text{b}},\text{H-3}^{\text{b}}}$ | | H2''-C2'-C3'-H3' | 86.4 | 0.6 | 6.7 | 83.9 | 0.7 | 6.7 | | |
| $^3J_{\text{H-3}^{\text{b}},\text{H-4}^{\text{b}}}$ | | H3'-C2'-C3'-H4' | -104.1 | 1.5 | 3.8 | -99.6 | 1.2 | 4.3 | | |
| $^3J_{\text{H-4}^{\text{b}},\text{H-5}^{\text{b}}}$ | | H4'-C2'-C3'-H5' | 56.2 | 1.1 | 2.7 | 57.2 | 1.0 | 4.9 | | |
| $^3J_{\text{H-4}^{\text{b}},\text{H-5}^{\text{b}}}$ | | H4'-C2'-C3'-H5'' | -64.5 | 2.0 | 5.5 | 178.6 | 10.2 | 3.0 | | |
| N (%) ^c | | | | 61 | | | 56 | | | |

^a HF/6-31G** basis set was used. ^b Coupling constants of the methyl group protons calculated as average of the individual $^3J_{\text{H,H}}$ coupling constants. ^c N (%) = $100(1 - (\sum J_{\text{H1}'} - 9.8)/5.9)$.^{42,43}

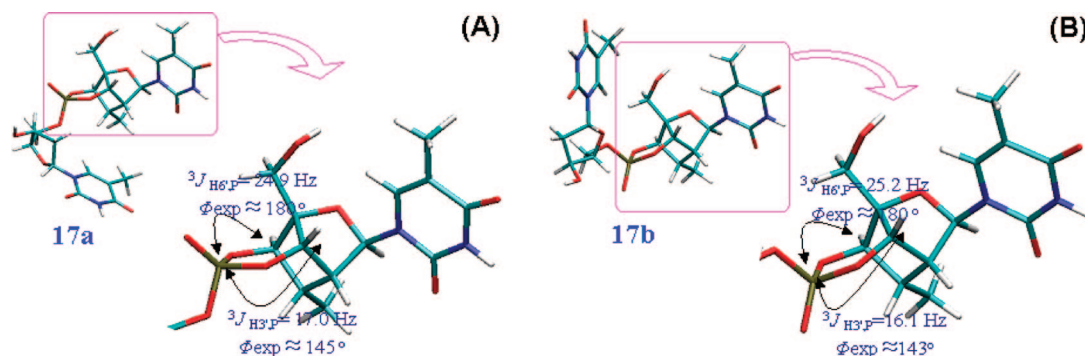


FIGURE 2. Ab initio geometry optimized structures of (S_{p})-D₂-CNA-dT **17a** (panel A) and (R_{p})-D₂-CNA-dT **17b** (panel B), which fulfill all NMR data (see Table 1). The part inside the pink frame was expanded to the right. The experimental torsion angles (Φ_{exp}) were calculated on the basis of the experimental $^3J_{\text{P,H}}$ employing the simplified Karplus equation $^3J_{\text{POCH}} = A \cos^2(\phi) + B \cos(\phi) + C$, where the $A = 15.3$; $B = -6.2$; $C = 1.5$ as in ref 48.

tion (Figure 2). Sugar and backbone torsions of constrained D₂-CNA at the 5'-end of (S_{p})-**17a** were found to be nearly identical to that of (R_{p})-**17b** (Table S1, Supporting Information). The torsion angles δ and ϵ were found to be constrained in *gauche*(+) (g^+ , 73.0°) and *cis* (7.5°) conformations for (S_{p})-**17a** and *gauche*(+) (g^+ , 72.2°) and *cis* (16.4°) conformations for (R_{p})-**17b**. The differences between (S_{p})-**17a** and (R_{p})-**17b** arise from two diastereotopic oxygen atoms of the phosphate. Thus, in (S_{p})-**17a**, the 3'-end nucleoside is attached to the axial oxygen of the 1,3,2-dioxaphosphorinane, and the ζ torsion adopts an *antiperiplanar*(+) (a^+ , 133.1°) conformation, which is compared to the *antiperiplanar*(-) (a^- , -98.3°) conformation of ζ in (R_{p})-**17b** whose 3'-nucleoside is attached to the equatorial oxygen.

Contrary to the rigidity of the sugar at the 5'-end of the D₂-CNA, the pentose sugars at the 3'-end nucleoside (dT) in **17a**

and **17b** are flexible (Table 1). To estimate the ratio of the North and South conformers of sugar in the experimental conditions, we have used the previously reported equation^{42,43} N (%) = $100(1 - (\sum J_{\text{H1}'} - 9.8)/5.9)$, which puts the fraction of North-type puckered nucleosides at the 3'-end to ~61% in compound (S_{p})-**17a** and to ~56% in (R_{p})-**17b**. These ratios of N/S-type sugar populations are quite different from the equilibrium observed in case of the native 2'-deoxynucleotides (30–40% North).⁴⁴ Thus, the presence of rigid tricyclic modification at the 5'-end does induce a change in the sugar conformation of the neighboring 3'-end nucleotide in these dimeric nucleotides.

The torsion angles of D₂-CNA-dT have been compared with those of other δ, ϵ, ζ constrained D-CNA-dT dimers (Table S2, Supporting Information). The major difference between D₂-CNA and other δ, ϵ, ζ -constrained D-CNA as well as native DNA is that D₂-CNA has a unique *cis* conformation across the torsion ϵ , while the torsion ϵ of others vary between a^+ , t , and a^- . The preferred *cis* conformation of torsion ϵ has never been found in

(41) Plashkevych, O.; Chatterjee, S.; Honcharenko, D.; Pathmasiri, W.; Chattopadhyaya, J. *J. Org. Chem.* **2007**, *72*, 4716–4726.

(42) Rinkel, L. J.; Altona, C. *J. Biomol. Struct. Dyn.* **1987**, *4*, 621–649.

(43) Isaksson, J.; Acharya, S.; Barman, J.; Cheruku, P.; Chattopadhyaya, J. *Biochemistry* **2004**, *43*, 15996–16010.

(44) Plavec, J.; Tong, W.; Chattopadhyaya, J. *J. Am. Chem. Soc.* **1993**, *115*, 9734–9746.

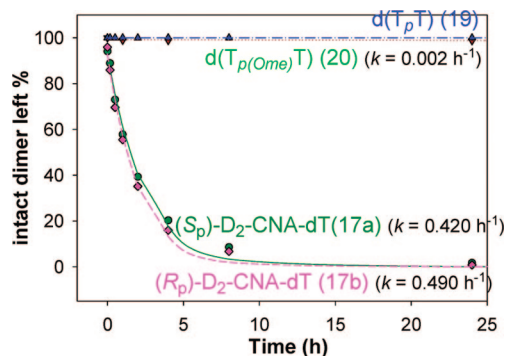


FIGURE 3. Digestion plots of (S_p)-D₂-CNA-dT dimer (**17a**), (R_p)-D₂-CNA-dT dimer (**17b**), native d(T_pT) (**19**), and d($T_{p(OMe)T}$) (**20**) under aqueous NaOH (1 mM) solution at room temperature.

the native as well as in other modified nucleotides. This unique structural feature of D₂-CNA makes it a valuable model to study conformation dependent processes such as RNA hydrolysis,⁴⁵ enzymatic phosphate transfer,⁴⁶ and protein–nucleic acid interactions.⁴⁷

3.0. Chemical Stability of (R_p)- and (S_p)-D₂-CNAs. **3.1. Stability of 1,3,2-Dioxaphosphorinane System in D₂-CNA in aq NaOH.** To test the stability of (R_p)- and (S_p)-D₂-CNA dimers **17a** and **17b** toward hydroxide ion, pure (R_p)- or (S_p)-D₂-CNA-dT dimer, the native dimer d(T_pT) (**19**) or methyl triester dimer d($T_{p(OMe)T}$) (**20**) was incubated with aqueous 1 mM NaOH solution at 21 °C. Aliquots were taken at regular time intervals and analyzed by HPLC (Figures S111–114, Supporting Information). The digestion plots of these dimers are shown in Figure 3. Under these conditions, native dimer d(T_pT) was completely stable, whereas consistent with the previous reports,^{49,50} the d($T_{p(OMe)T}$) (**20**) decomposed slowly under these conditions (pseudo-first-order reaction rate $k = 0.002 \text{ h}^{-1}$). In contrast, the cyclic phosphotriester function in (S_p)-D₂-CNA-dT (**17a**) ($k = 0.42 \text{ h}^{-1}$) is somewhat more stable than (R_p)-D₂-CNA-dT (**17b**) ($k = 0.49 \text{ h}^{-1}$), but both **17a** and **17b** were nearly 200 times more labile than d($T_{p(OMe)T}$) (**20**). This result suggests that the conformationally constrained phosphotriesters in **17a** and **17b** are much more unstable toward nucleophile than conformation unconstrained phosphotriesters (as in **20**), which is consistent with the relative faster rate of hydrolysis of simple cyclic phosphotriesters compared to the acyclic counterpart⁵¹ because of the ring-strain in the former.

3.2. Characterization of Decomposition Products from the Alkaline Digestion of D₂-CNA **17a and **17b**.** After 24 h incubation in 1 mM NaOH aqueous solution, both (S_p)-D₂-CNA-dT **17a** and (R_p)-D₂-CNA-dT **17b** were digested completely and gave three detectable products: carba-LNA-6',5'-dT (**21**), carba-LNA-3',5'-dT (**22**), and carba-LNA-6',3'-dT (**23**) (NMR characterization of these three products is shown in the Experimental Section and Supporting Information; the structures of compounds **21–23** are shown in Figure 4). For (S_p)-**17a**, the relative

ratio of compounds **21:22:23** is 74:8:18, and for (R_p)-**17b**, the relative ratio of the products **21:22:23** is 86:10:4. Hence, upon attack by hydroxide on phosphorus in **17a** and **17b**, scission of the P -3' aO bond is always the major reaction pathway to give the major product, carba-LNA-6', 5'-dT (**21**). Product **22**, which was formed by scission of bond P -6' aO , can also be observed, but it was only about 10%. The third product, carba-LNA-6', 3'-dT (**23**), could have been formed through intramolecular attack by the 3' $b-O^-$ on phosphorus accompanied by capture of 6' $a-O^-$. Scission of the P -5' bO bond which leads to chain cleavage was not observed here.

Upon intermolecular nucleophilic attack, scission of the P -3' aO bond/ P -6' aO bond/ P -5' bO bond is generally in the ratio of 90/10/0 for both (S_p)-**17a** and (R_p)-**17b**, which corroborate the conclusion that it is the ring strain that makes the D₂-CNA extremely unstable toward strong nucleophiles, and moreover, this result also suggests that in D₂-CNA, the 3' aO^- anion is a much better leaving group and thus much more electronegative than 6' aO^- .

3.3. Stability of 1,3,2-Dioxaphosphorinane System in D₂-CNA in Concentrated Aqueous Ammonia. The stability of D₂-CNA-dT dimers **17a** and **17b** in concentrated aqueous ammonia at room temperature was also studied. It was found that, under these conditions, the $t_{1/2}$ of hydrolysis of the phosphotriester in (S_p)-D₂-CNA-dT dimer **17a** and (R_p)-D₂-CNA-dT dimer **17b** are 12 and 6 min, respectively (Figure 5A). Hence, (R_p)-D₂-CNA is two times more labile than (S_p)-D₂-CNA. The degradation products from both dimers and their relative ratios of the products (**21/22/23**) were still approximately the same in aq NaOH hydrolysis as in the dimer (S_p)-**17a** and gave **21:22:23** in a 75:14:11 ratio, whereas the dimer (R_p)-**17b** gave **21:22:23** in a 91:8:2 ratio (Figures S115 and S116, Supporting Information).

3.4. Stability of 1,3,2-Dioxaphosphorinane System in D₂-CNA in 0.5 M Hydrazine Hydrate in Pyridine/AcOH (4/1, v/v). To test the stability of each of the pure diastereomeric D₂-CNAs toward weak nucleophile under neutral conditions, (S_p)-D₂-CNA-dT dimer **17a** and (R_p)-D₂-CNA-dT dimer **17b** were incubated with 0.5 M hydrazine hydrate in pyridine/AcOH (4/1, v/v, pH = 5.6⁵²) at 21 °C. From Figure 5B, it can be seen that under these conditions, (S_p)-D₂-CNA **17a** was approximately two times more stable with $t_{1/2}$ of 178 h than that of (R_p)-D₂-CNA **17b** ($t_{1/2} = 99 \text{ h}$). It is noteworthy that we have subsequently exploited this relative stability in the deprotection of (S_p)-D₂-CNA containing oligonucleotides (see section 6.1).

3.5. Stability of 1,3,2-Dioxaphosphorinane System in D₂-CNA in 0.5 M DBU/MeCN. It was important to examine the stability of the 1,3,2-dioxaphosphorinane system in D₂-CNA toward a relatively strong non-nucleophilic organic base such as DBU, which was subsequently used to remove oligos from the solid support (see section 6.1).⁵³ Thus, (S_p)-D₂-CNA-dT dimer **17a** or (R_p)-D₂-CNA-dT dimer **17b** was incubated with 0.5 M DBU in dry MeCN at 21 °C. The digestion plots (Figure 5C) showed that both (S_p)-**17a** ($t_{1/2} = 154 \text{ h}$) and (R_p)-**17b** ($t_{1/2} = 330 \text{ h}$) degraded very slowly under these conditions. Since oligos can be cleaved from solid support in 24 h, the phosphotriester function in **17a** and **17b** will be expected to cleave less than 10% under these conditions.

(45) Soukup, G. A.; Breaker, R. R. *RNA* **1999**, *5*, 1308–1325.

(46) Cleland, W. W.; Hengge, A. C. *Chem. Rev.* **2006**, *106*, 3252–3278.

(47) Rice, P. A.; Correll, C. C. *Protein-Nucleic Acid Interactions: Structure Biology*; RSC Publishing: Cambridge, UK, 2008.

(48) Plavec, J.; Chattopadhyaya, J. *Tetrahedron Lett.* **1995**, *36*, 1949–1952.

(49) Shooter, K. V.; Merrifield, R. K. *Biochim. Biophys. Acta* **1978**, *521*, 155–159.

(50) Shooter, K. V. *Chem. Bio. Interactions* **1976**, *13*, 151–163.

(51) Dennis, E. A.; Westheimer, F. H. *J. Am. Chem. Soc.* **1966**, *88*, 3432–3433.

(52) Letsinger, R. L.; Miller, P. S.; Grams, G. W. *Tetrahedron Lett.* **1968**, *9*, 2621–2624.

(53) Brown, T.; Pritchard, C. E.; Turner, G.; Salisbury, S. A. *J. Chem. Soc., Chem. Commun.* **1989**, 891–893.

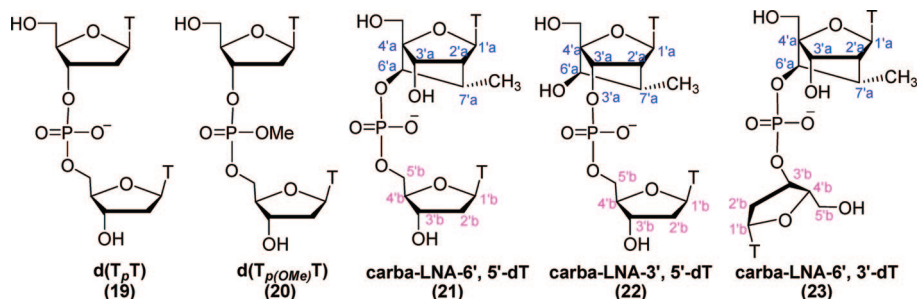


FIGURE 4. Structure of dimer d(T_pT) (19), d(T_{p(OMe)}T) (20), carba-LNA-6', 5'-dT (21), carba-LNA-3', 5'-dT (22), and carba-LNA-6', 3'-dT (23).

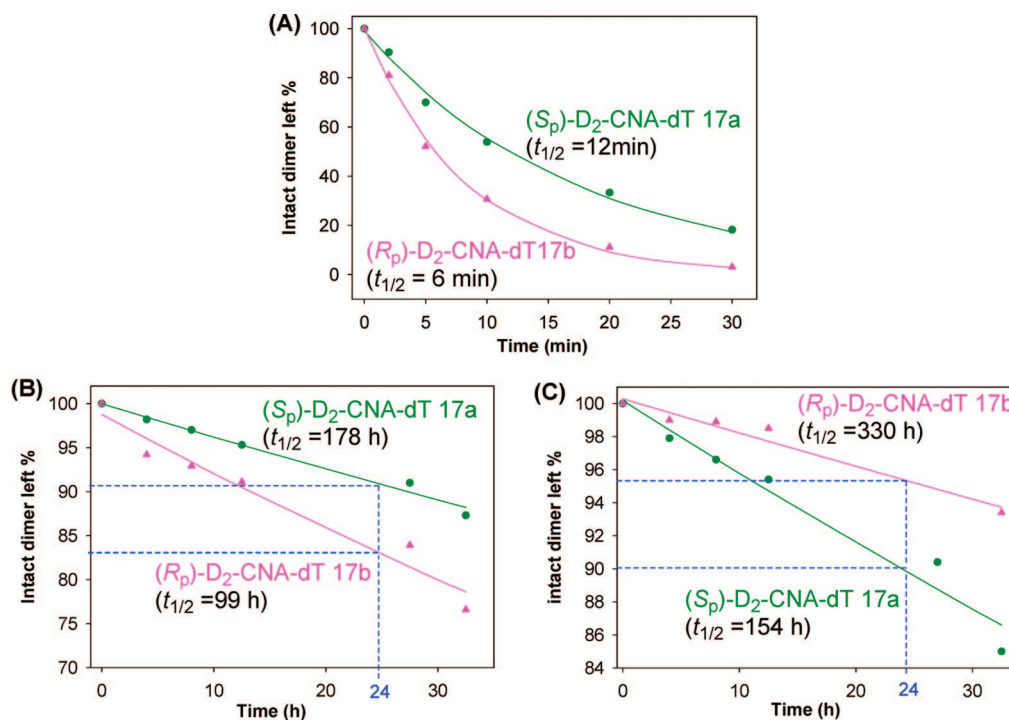


FIGURE 5. Digestion plots of (S_p)-D₂-CNA-dT dimer 17a and (R_p)-D₂-CNA-dT dimer 17b under different conditions. (Panel A): in concentrated aqueous ammonia. (Panel B): in 0.5 M hydrazine hydrate in pyridine/AcOH (4/1, v/v). (Panel C): in 0.5 M DBU/MeCN.

4.0. Nuclease Stability of D₂-CNA. It is known that 2'-deoxyoligonucleotides with a methyl phosphotriester function are resistant to nuclease digestion.⁵⁴ To test the stability of dioxaphosphorinane system in D₂-CNA toward nuclease, (S_p)-D₂-CNA-dT dimer 17a, (R_p)-D₂-CNA-dT dimer 17b, as well as d(T_pT) (19) and d(T_{p(OMe)}T) (20) were treated with snake venom phosphodiesterase (SVPDE). Aliquots were taken at regular time points and analyzed by HPLC (Figures S121–S124, Supporting Information). The digestion plots are shown in Figure 6. The native DNA dimer d(T_pT) was digested by SVPDE very fast (t_{1/2} = 31 min), whereas D₂-CNA 17a, 17b and dT_{p(OMe)}dT were completely stable up to 2 h. Thus, the conformationally constrained phosphotriesters D₂-CNA, just like the methyl triester nucleotides, are resistant to nuclease digestion.

5.0. Fluoride-Mediated Equilibration between the Diastereomeric Pairs of (R_p)-16b and (S_p)-16a. **5.1. Reaction of F⁻ Ion with (R_p)-16b and (S_p)-16a.** Thus, when pure (R_p)-16b was dissolved in dry THF-*d*₈ and kept in an NMR tube at 25 °C for 24 h, it was found to be completely stable without showing any sign of isomerization, as evidenced by ¹H and ³¹P

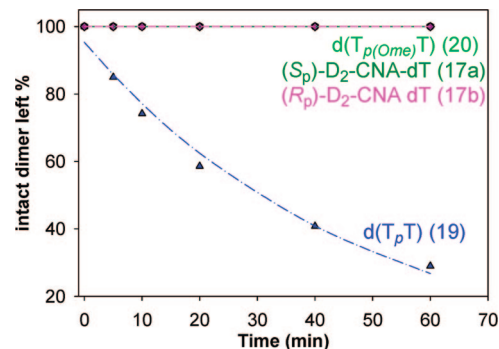


FIGURE 6. Digestion plots of d(T_pT) (19), d(T_{p(OMe)}T) (20), (S_p)-D₂-CNA-dT dimer 17a, and (R_p)-D₂-CNA-dT dimer 17b with SVPDE. Digestion conditions: Dimer 1 O.D. (A_{260nm}), 100 mM Tris-HCl (pH 8.0), 15 mM MgCl₂, SVPDE 3 μg/mL, total reaction volume 1 mL.

NMR (Figure 7A,B). Subsequently, after 24 h at rt, 1 equiv of dry TBAF in THF was added and the reaction mixture was examined at different time intervals by ¹H and ³¹P NMR. The NMR showed the appearance of the resonances from compound (S_p)-16a in addition to the starting (R_p)-16b. By integration of the H1'a peaks of (S_p)-16a and (R_p)-16b in ¹H NMR, it was

(54) Miller, P. S.; Fang, K. N.; Kondo, N. S.; Ts'o, P. O. P. *J. Am. Chem. Soc.* **1971**, *93*, 6657–6665.

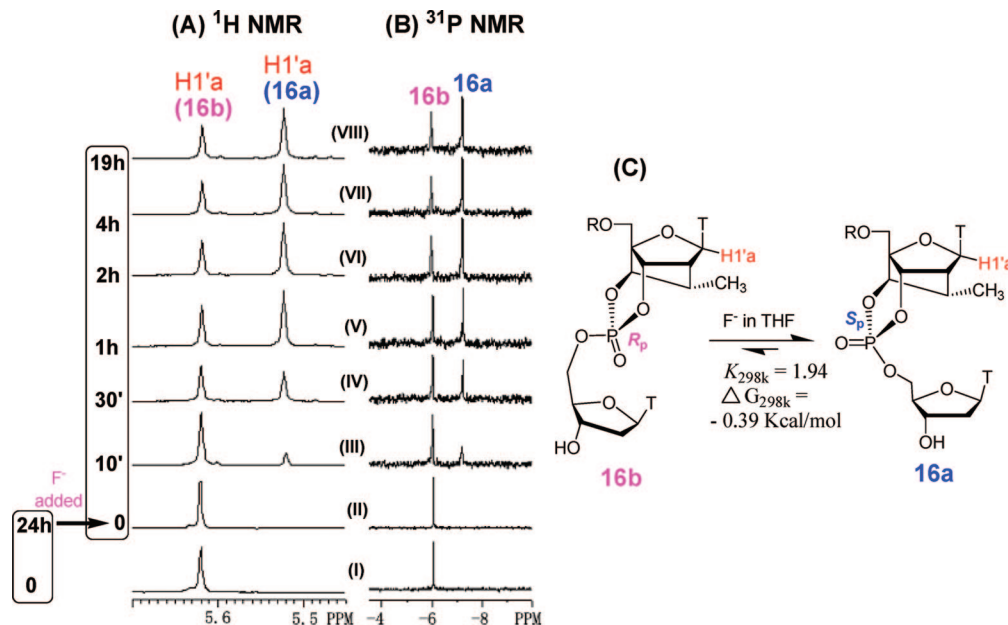


FIGURE 7. Fluoride-catalyzed isomerization between (*S_p*)-**16a** and (*R_p*)-**16b**. Pure **16b** was dissolved in dry THF-*d*₈ in an NMR tube (I). It was first kept at 25 °C for 24 h (II), and then 1 equiv of dry TBAF in THF was added. ¹H NMR (H1'a region in panel A) and ³¹P NMR (in panel B) of this sample were monitored at regular time intervals (III–VIII).

found that as the amount of (*R_p*)-**16b** decreased with time, the amount of (*S_p*)-**16a** gradually increased. After 2 h, the ratio of (*R_p*)-**16b**/*S_p*-**16a** (66:34) did not change for up to 19 h, thereby showing that they have reached an equilibrium giving an equilibrium constant, $K_{298\text{K}} = 1.92$, which corresponds to $\Delta G_{298\text{K}} = -0.39$ kcal/mol (Figure 7C).

5.2. Axial Isomer *S_p*-16a** Is Only 0.39 kcal/mol More Stable than the Equatorial Isomer *R_p*-**16b** and Hydrolysis of *R_p*-**17b** Is Faster than *S_p*-**17a** Only by a Factor of 2. Why?** It has been previously established that an electronegative substituent on phosphorus in a 2-oxo-1,3,2-dioxaphosphorinane prefers the axial orientation at ambient temperature.³⁷ This means that the axial isomer is more thermally stable than the equatorial isomer. Gorenstein et al. have reported that equatorial isomers are 1.45–1.95 kcal/mol more stable than the equatorial counterparts and the hydrolysis of equatorial isomers were relatively faster by a factor of 3–9.⁵⁵ We have, however, observed that *S_p*-**16a** (axial isomer) is only 0.39 kcal/mol more stable than *R_p*-**16b** (equatorial isomer) and hydrolysis of *R_p*-**17b** was only faster than *S_p*-**17a** by a factor of 2 (see section 3.0). The comparatively lower energy difference and smaller hydrolysis rate variation between axial isomer *S_p*-CNA and equatorial isomer *R_p*-CNA could be attributed to the unique conformationally constrained nature of the dioxaphosphorinane ring in *S_p*-CNA and *R_p*-CNA. As we have already established in section 2.0, the six-membered dioxaphosphorinane ring adopts an imperfect half-chair conformation and the exocyclic alkoxy substituents occupies the pseudoaxial or pseudoequatorial position in *S_p*-**17a** and *R_p*-**17b**, respectively. The pseudoequatorial orientation of alkoxy substituents could exert a stabilization effect for *R_p*-**16b** because of the anomeric effect.^{55–57} On the other hand, pseudoaxial orientation of alkoxy substituents could lead to a destabilization of *S_p*-**16a** because of the competing steric effect, and thus, this balancing act between

anomeric and steric effects optimizes the energy difference between *S_p*-**16a** and *R_p*-**16b** diastereomers.

5.3. Plausible Mechanism of Fluoride Ion Catalyzed Isomerization between (*S_p*)-16a** and (*R_p*)-**16b**.** The fluoride-catalyzed isomerization between (*S_p*)-**16a** and (*R_p*)-**16b** is expected to take place through two successive nucleophilic attacks. This process starts by F⁻ attack on phosphorus with development of the trigonal-bipyramidal intermediates. In these intermediates, F takes up an apical position, and the second apical position could be occupied by 3'aO, 6'aO, or 5'bO through path A, B, or C, respectively (Figure 8). From path A, trigonal-bipyramidal intermediate **Ts-A1** was obtained, in which both 3'aO and 6'aO from the 6-membered dioxaphosphorinane ring occupy equatorial positions and it is energetically unfavorable.⁵⁸ Moreover, scission of the P-5'bO bond in **Ts-A1** will lead to chain cleavage. Actually, no trace of chain cleavage products could be observed in the NMR spectra of the fluoride-catalyzed isomerization study, which is also consistent with the reaction we have studied with the hydroxide ion as nucleophile (see section 3.2). Thus, we concluded that path A cannot be included in the isomerization process. From path B, trigonal-bipyramidal intermediate **Ts-B1** was obtained in which the 3'aO can occupy the apical position. If 3'aO⁻ is a direct departing group, phosphorofluoridate **TS-B3** will be formed. This phosphorofluoridate is not stable.^{59,60} The intramolecular attack by 3'aO⁻ to phosphorus in line with F takes place very fast,⁶¹ and as a result, the starting material **16b** was obtained. Thus, the process (*R_p*)-**16b** ⇌ **Ts-B1** ⇌ **TS-B3** ⇌ (*R_p*)-**16b**, which is composed of two successive in-line attacks, only leads to the chiral retention product. On the other hand, if a pseudorotation process takes place in **Ts-B1**, **Ts-B2** will be obtained. In **Ts-B2**, the apically occupied 6'aO⁻ departs to give phosphorofluoridate **TS-B4**, and then 6'aO⁻ attacks the phosphorus in-line with F

(58) Day, R. O.; Kumara Swamy, K. C.; Fairchild, L.; Holmes, J. M.; Holmes, R. R. *J. Am. Chem. Soc.* **1991**, *113*, 1627–1635.

(59) Misiura, K.; Pietrasiak, D.; Stec, W. J. *J. Chem. Soc., Chem. Commun.* **1995**, 613–614.

(60) Sund, C.; Chattopadhyaya, J. *Tetrahedron* **1989**, *45*, 7523–7544.

(61) Baraniak, J.; Stec, W. J. *Tetrahedron Lett.* **1995**, *36*, 8119–8122.

(55) Gorenstein, D. G.; Rowell, R.; Findlay, J. *J. Am. Chem. Soc.* **1980**, *102*, 5077–5088.

(56) Bailey, W.; Eliel, E. *J. Am. Chem. Soc.* **1974**, *96*, 1798–1806.

(57) Gorenstein, D. G.; Kar, D. *J. Am. Chem. Soc.* **1977**, *99*, 672–677.

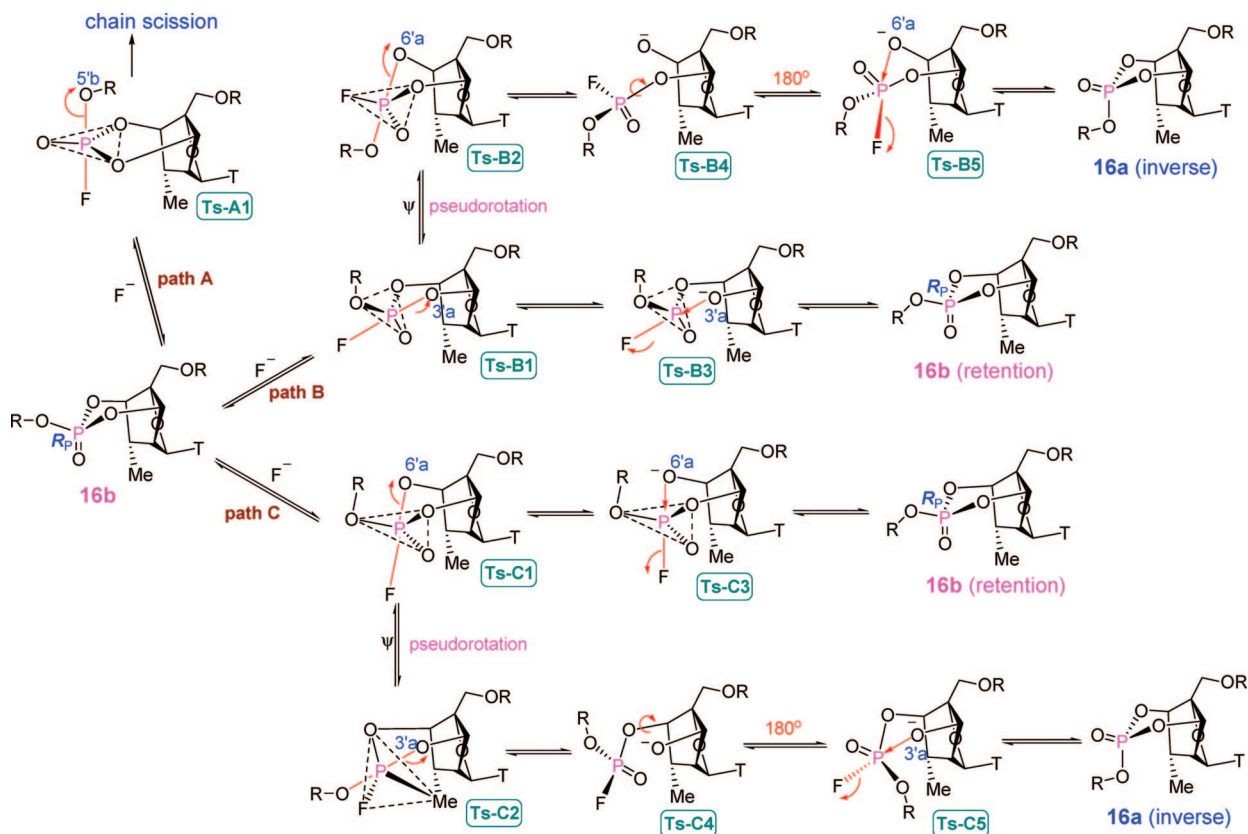


FIGURE 8. Plausible mechanism of fluoride ion catalyzed isomerization between (S_p)-**16a** and (R_p)-**16b**, supporting the nature of products formed and isolated as well as their experimental distribution (see section 3.0).

(**TS-B5**) to give (S_p)-**16a**. Thus, the process (R_p)-**16b** \rightleftharpoons **Ts-B1** \rightleftharpoons **Ts-B2** \rightleftharpoons **Ts-B4** \rightleftharpoons **Ts-B5** \rightleftharpoons (S_p)-**16a**, which is composed of two in-line attacks plus one intermediary pseudorotation, can give chiral inverted product (S_p)-**16a** from (R_p)-**16b**. This explains why pure (R_p)-**16b** gives (S_p)-**16a**.

Similarly, (S_p)-**16a** can also be obtained from (R_p)-**16b** through path **C** by successive in-line attack, pseudorotation, and in-line attack (R_p)-**16b** \rightleftharpoons **Ts-C1** \rightleftharpoons **Ts-C2** \rightleftharpoons **Ts-C4** \rightleftharpoons **Ts-C5** \rightleftharpoons (S_p)-**16a**). It is known that in the trigonal-bipyramidal intermediate, electronegative ligands prefer the apical position.^{62,63} From section 3.2, we have also learned that the oxanion charge is more strongly localized on 3'aO because it is relatively more electronegative than 6'aO, and hence, trigonal-bipyramidal intermediate **Ts-B1** from path **B**, in which 3'aO takes up the apical position, is more favorable than **Ts-C1** from path **C** in which 6'aO takes up the apical position. Thus, either (S_p)-**16a** or (R_p)-**16b** can interconvert to each other through the mediation F ion to reach an equilibrium, most probably through path **B** as the major pathway and path **C** as the minor pathway. These conclusions are consistent with the experimentally observed hydroxide ion promoted cleavage of (S_p)-**16a** and (R_p)-**16b** phosphotriesters to give carba-LNA-6',5'-dT (**21**) (90%) and carba-LNA-3',5'-dT (**22**) (10%).

6.0. Incorporation of Diastereomerically Pure D₂-CNA into AONs and Thermal Denaturation Studies. 6.1. Synthesis of (S_p)-D₂-CNA-Substituted Oligonucleotides. In order to incorporate the D₂-CNA-dT dimer into antisense oligodeoxynucleotide (AON), the more stable, major diastereomer 5'a-

DMTr-(S_p)-D₂-CNA-dT **16a** was used to synthesize the corresponding phosphoramidite **18** (Scheme 3) in 70% yield according to standard procedure.⁶⁴ Using phosphoramidite **18**, four DNA sequences AONs **2–5** (Table 2) were synthesized on the basis of solid-supported DNA synthesis technology. The solid support was commercially available succinyl-LCAA-CPG, and the UltraMILD native phosphoramidite monomers (Pac-dA, Ac-dC) were used. The coupling yield for phosphoramidite **18** varied from 50–60%.

Since we have found in our model study (section 3.5) that the internucleotidic phosphotriester in D₂-CNA was stable in the presence of DBU in CH₃CN at rt, we used the 0.5 M DBU in dry MeCN⁵³ to cleave oligonucleotides from succinyl-LCAA-CPG solid support. Also, because of the stability of the internucleotidic phosphotriester in our model compounds (section 3.4) under 0.5 M hydrazine hydrate in pyridine/AcOH (4/1, v/v), we could successfully employ this condition^{65,66} to deprotect the protecting groups on adenine and cytosine from our AONs.

Thus, the solid supports of AONs **2–5** were first treated with Et₃N/MeCN (3/2, v/v) for 2 h to remove the cyanoethyl group on the phosphate linkage,⁶⁷ then treated with 0.5 M DBU in dry MeCN for 24 h to cleave the oligos from the solid support, and finally treated with 0.5 M hydrazine hydrate in pyridine/AcOH (4/1, v/v) for 24 h at rt to remove the protecting groups

(64) Zhou, C.; Honcharenko, D.; Chattopadhyaya, J. *Org. Biomol. Chem.* **2007**, *5*, 333–343.

(65) van Boom, J. H.; Burgers, P. M. J. *Tetrahedron Lett.* **1976**, *17*, 4875–4878.

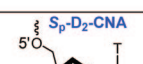
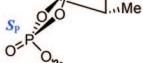
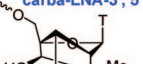
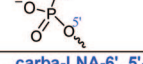
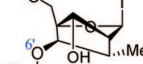
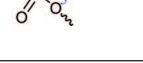
(66) Iwai, S.; Ohtsuka, E. *Nucleic Acids Res.* **1988**, *16*, 9443–9456.

(67) Eritja, R.; Robles, J.; Fernandez-Fornier, D.; Albericio, F.; Giral, E.; Pedrosa, E. *Tetrahedron Lett.* **1991**, *32*, 1511–1514.

(62) Westheimer, F. H. *Acc. Chem. Res.* **1968**, *1*, 70–78.

(63) Oivanen, M.; Kuusela, S.; Lönnberg, H. *Chem. Rev.* **1998**, *98*, 961–990.

TABLE 2. Thermal Denaturation of Duplexes of Native and Modified AONs with complementary RNA or DNA^a

| Entry | Structure of modifications | Sequence | (MH) ⁺ | | With RNA | | With DNA | |
|---------------------|---|----------------------------|-------------------|--------|----------|--------------|----------|--------------|
| | | | Cacl. | Found | T_m | ΔT_m | T_m | ΔT_m |
| AON 1 | | 3'-d (CTT CTT TTT TAC TTC) | 4448.7 | 4449.7 | 44.4 | | 44.8 | |
| AON 2 |  | 3'-d (CTT CTT TTT TAC TTC) | 4486.8 | 4487.2 | 39.9 | -4.5 | 42.7 | -2.1 |
| AON 3 | | 3'-d (CTT CTT TTT TAC TTC) | 4486.8 | 4487.1 | 37.7 | -6.7 | 37.7 | -7.1 |
| AON 4 | | 3'-d (CTT CTT TTT TAC TTC) | 4486.8 | 4487.1 | 37.0 | -7.4 | 35.8 | -9.7 |
| AON 5 |  | 3'-d (CTT CTT TTT TAC TTC) | 4486.8 | 4487.2 | 37.6 | -6.8 | 37.6 | -7.2 |
| AON 6 ^b |  | 3'-d (CTT CTT TTT TAC TTC) | 4504.6 | 4504.8 | 47.6 | +2.9 | 47.1 | +1.6 |
| AON 7 ^b | | 3'-d (CTT CTT TTT TAC TTC) | 4504.6 | 4505.4 | 48.8 | +4.1 | 46.0 | +0.5 |
| AON 8 ^b | | 3'-d (CTT CTT TTT TAC TTC) | 4504.6 | 4505.1 | 48.9 | +4.2 | 45.4 | -0.1 |
| AON 9 ^b |  | 3'-d (CTT CTT TTT TAC TTC) | 4504.6 | 4505.5 | 48.3 | +3.6 | 44.2 | -1.3 |
| AON 10 ^c |  | 3'-d (CTT CTT TTT TAC TTC) | 4504.6 | 4505.1 | 38.6 | -5.8 | 39.0 | -5.8 |
| AON 11 | | 3'-d (CTT CTT TTT TAC TTC) | 4504.6 | 4505.4 | 33.9 | -10.5 | 27.7 | -17.1 |
| AON 12 ^c | | 3'-d (CTT CTT TTT TAC TTC) | 4504.6 | 4505.0 | 33.6 | -10.8 | 25.3 | -19.5 |
| AON 13 ^c |  | 3'-d (CTT CTT TTT TAC TTC) | 4504.6 | 4505.5 | 32.4 | -12.0 | 26.5 | -18.3 |

^a T_m values measured as the maximum of the first derivative of the melting curve ($A_{260\text{nm}}$ vs temperature) in medium salt buffer (60 mM Tris-HCl at pH 7.5, 60 mM KCl, 0.8 mM MgCl₂) with a temperature range of 18–60 °C using 1 μM concentrations of the two complementary strands. The value of T_m given is the average of two or three independent measurements. If error of the first two measurements is deviated from ± 0.3 °C, the third measurement was carried out to confirm if the error is indeed within ± 0.3 °C. ^b AONs 6–9 have been reported in our previous paper,³⁰ and here they are used as standards for comparison. ^c The samples of AON 10, AON 12, and AON 13 were contaminated with about 20% of AON 6, AON 8, and AON 9, respectively. ^d T_m inside the parentheses are the second transition (higher T_m , Figure 10B) observed on the melting curves. It corresponds to T_m 's of impurity of AON 8 in the sample of AON 12. ^e T_m inside the parentheses are the second transition (higher T_m , Figure 10B) observed on the melting curves. It corresponds to T_m 's of impurity of AON 9 in the sample of AON 13.

on the nucleobases to give the crude oligonucleotides, which were purified by RP-HPLC to give pure AONs 2–5 (Figure S125, Supporting Information) in 35–40% yield. The integrity of structures of AONs 2–5 has been verified by the MALDI-TOF mass measurements. Thus, mass of pure AONs 2–5 were observed at m/z 4487 for the molecular weight, $[\text{MH}]^+ = 4486.8$, thereby suggesting that the sensitive internucleotidyl six-membered 1, 3, 2-dioxaphosphorane ring in (S_p)-D₂-CNA-modified AONs 2–5 have been kept intact during the deprotection conditions, because if the internucleotidyl 1,3,2-dioxaphosphorinane ring opened up by hydrolysis, the $[\text{MH}]^+$ of the oligos would have been at m/z 4505 because of addition of 1 mol of water. One example of comparative molecular weight of AON 3 with full phosphotriester function intact and its 6',5'- and 3',5'-hydrolyzed product (purified) is shown in Figure 9. The MALDI-TOF mass measurements of other (S_p)-D₂-CNA modified oligos are shown in the Supporting Information (Figure S130–S133), and they all show that the phosphotriester moiety in each of them is indeed intact.

6.2. Thermal Denaturation Studies of Duplexes Formed by AONs 1–5 with Complementary RNA or DNA. The T_m values of duplexes formed by AONs 1–5 with complementary RNA or DNA are listed in Table 2, and melting curves of AONs with complementary RNA are shown in Figure 10A. The (S_p)-D₂-CNA affects the thermal stability of AON/RNA duplex in a sequence-dependent manner. When located at the end of the AON sequence as in AON 2, generally, it destabilizes the AON/RNA duplex by -4.5 °C/modification compared to the native counterpart AON 1, whereas when it is located in the middle of AON sequences, as in AONs 3–5 modifications, it exerts a much more negative effect (ca. -7 °C/modification) for the thermal stability of AON/RNA duplex. Moreover, the (S_p)-D₂-CNA modified AONs 3–5 are RNA selective; thus, AON/RNA generally have higher T_m than AON/DNA duplex.

It is known from our previous work that carba-LNA-3',5'-phosphodiester-modified AONs 6–9 thermally stabilize the AON/RNA duplex by about $+4$ °C/modification.³⁰ Compared to carba-LNA-3',5'-phosphodiester, the (S_p)-D₂-CNA has a neutral phosphotriester linkage, which is expected to stabilize AON/RNA or AON/DNA duplexes because the repulsion of negative charge on phosphate between strands is minimized. Hence, we argued that (S_p)-D₂-CNA could make a geometry distortion in AON/RNA and AON/DNA duplexes because of the formation of C6'O–P bond, which could explain why (S_p)-D₂-CNA destabilize both AON/RNA and AON/DNA duplexes. In order to prove this hypothesis, we have synthesized carba-LNA-6',5'-phosphodiester modified AONs 10–13 and compared their thermal denaturation properties with (S_p)-D₂-CNA containing AONs 2–5 and carba-LNA-3',5'-phosphodiester-modified AONs 6–9.

6.3. Synthesis of Carba-LNA-6',5'-phosphodiester Containing AONs. It is stated above (see section 3.3) that the $t_{1/2}$ of ring-opening of dioxaphosphorinane system in (S_p)-D₂-CNA is 12 min (Figure 5A) in concentrated ammonia. Under this condition, the $t_{1/2}$ of deprotecting the *N*-Pac group from adenine has been reported to be 7 min⁶⁸ and $t_{1/2}$ of cleavage of oligos from succinyl-CPG is about 20 min.⁶⁹ Hence, we anticipated that if aqueous ammonia is used as the deprotection reagent, the 1,3,2-dioxaphosphorinane ring of D₂-CNA in the AON should be completely decomposed, giving carba-LNA-6',5'-phosphodiester and carba-LNA-3',5'-phosphodiester as observed in section 3.3. Thus, after treatment of solid supports of AONs 2–5 with 33% aqueous ammonia at room temperature for 4 h, crude products of carba-LNA-6',5'-modified AONs 10–13 were obtained, which were contaminated with small amounts of carba-

(68) Schulhof, J. C.; Molkl, D.; Teoule, R. *Nucleic Acids Res.* **1987**, *15*, 397–416.

(69) Reddy, M. P.; Hanna, N. B.; Farooqui, F. *Tetrahedron Lett.* **1994**, *35*, 4311–4314.

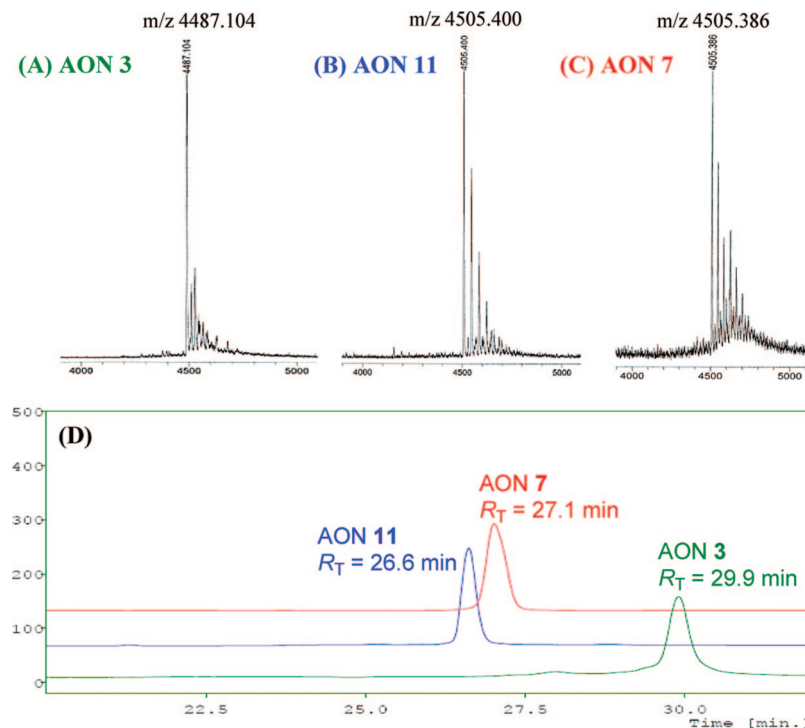


FIGURE 9. MALDI-TOF mass spectra of pure AON 3 (panel A, $[MH^+]$ found at m/z 4487.104, calcd 4486.8). Treatment of AON 3 with ammonia leads to 1,3,2-dioxaphosphorinane ring opening, giving 6',5'-phosphodiester modified AON 11 as the major hydrolyzed product (83%) with 17% of minor hydrolyzed product AON 7 (3',5'-phosphodiester modified, see section 6.3). Note that the mass spectra shown are for pure isomeric AON 11 (panel B) and AON 7 (panel C). Both the isomeric AON 11 and AON 7 have m/z at 4505 because of addition of 1 mol of water to the parent phosphotriester in AON 3. Panel D shows the HPLC profiles of pure AON 3, AON 7, and AON 11. HPLC conditions: reversed-phase (RP) HPLC: Kromasil 100, C18, 5 μ m, 250 \times 8 mm. 0–40', A \rightarrow A/B = 60/40, v/v. Flow of 1.5 mL/min at room temperature was used in a UV detector with detecting wavelength of 260 nm. For the HPLC purity as well as MALDI-TOF mass spectra of other pure (S_p)-D₂-CNA modified AONs 2, 4, and 5, see the Supporting Information (Figures S130–S133).

LNA-3',5'-modified AONs 6–9, as expected. Thus, the RP-HPLC analysis of the crude product of AON 11, upon ammonia treatment, was found to consist of two components (Figure S126A, Supporting Information), and both of them have $[MH]^+$ at 4505, corresponding to isomeric AON 11 and AON 7. Coinjection of the minor component with a standard sample of AON 7 (pure AONs 6–9 have been obtained using 6'*R*-OTol, 7'*S*-methyl-carba-LNA phosphoramidite in our previous report³⁰) showed that they were identical (Figure S126E, Supporting Information), so the minor component was AON 7 and the major component was putatively assigned as AON 11 because of identical mass as that of AON 7 (AON 11/ AON 7 = 83/17). This is fully consistent with our observation (see section 3.3) that the treatment of (S_p)-D₂-CNA-dT dimer 17a with aqueous ammonia gave carba-LNA-6', 5'-dT (21)/carba-LNA-3', 5'-dT (22) = 84/16. Hence, we conclude that both at the dimer level as well as in the oligomeric level, the internucleotidyl dioxaphosphorinane ring of D₂-CNA opened up hydrolytically, upon aqueous ammonia treatment, to give isomeric carba-LNA-6',5'-phosphodiester and carba-LNA-3',5'-phosphodiester in about 80/20 ratio. We could verify this isomerization reaction only for AON 11 with AON 7, but not for AON 10 with AON 6, AON 12 with AON 8, or AON 13 with AON 9 because of separation problem (Figures S127–129, Supporting Information). Hence, after purification by RP-HPLC, the AON 11 was obtained in the pure form, whereas the isolated AON 10, AON 12, and AON 13 were contaminated with about 20% of AON 6, AON 8, and AON 9, respectively, which is reflected in the T_m studies shown in Figure 10B.

6.4. Thermal Denaturation Studies of Carba-LNA-6',5'-phosphodiester-Modified AONs 10–13. The carba-LNA-6',5'-phosphodiester-modified pure AON 11 exert a higher thermal destabilization effect (-10.5 $^{\circ}$ C /modification) on the AON/RNA duplex. The samples of AON 10, AON 12, and AON 13 are contaminated with about 20% of AON 6, AON 8, and AON 12, respectively, and so in their melting curves especially for AON 12 and AON 13 two transitions can be observed (Figure 10B). The first transition (lower T_m) corresponds to the dissociation of AON 12 or AON 13 from RNA, and the second transition (higher T_m) corresponds to dissociation of impurity AON 8 or AON 10 from RNA. Like in AON 11, carba-LNA-6',5'-phosphodiester modifications in AON 12 and AON 13 also destabilize the AON/RNA by -10 to -12 $^{\circ}$ C /modification.

6.5. Determination of Relative Stacking Properties through Comparative CD Studies of Native Dimers d(T_pT) (19), (S_p)-D₂-CNA-dT (17a), Carba-LNA-3',5'-dT (22), and Carba-LNA-6', 5'-dT (21) To Explain Why Their Corresponding AON/DNA and AON/RNA Duplexes Have Such Different Thermal Stability. Circular dichroic (CD) spectroscopy has been extensively used to study the conformation of nucleic acid⁷⁰ in both the duplex form and single strand form⁷¹ or even in dinucleotide level.^{54,72,73} Ts'o et al. have reported that at the

(70) Gray, D. M.; Ratliff, R. L.; Vaughan, M. R. *Meth. Enzymol.* **1992**, *211*, 389–406.

(71) Powell, M. D.; Gray, D. M. *Biochemistry* **1993**, *32*, 12538–12547.

(72) Brahms, J.; Maurizot, J. C.; Michelson, A. M. *J. Mol. Biol.* **1967**, *25*, 481–495.

(73) Kondo, N. S.; Holmes, H. M.; Stempel, L. M.; Ts'o, P. O. P. *Biochemistry* **1970**, *9*, 3479–3498.

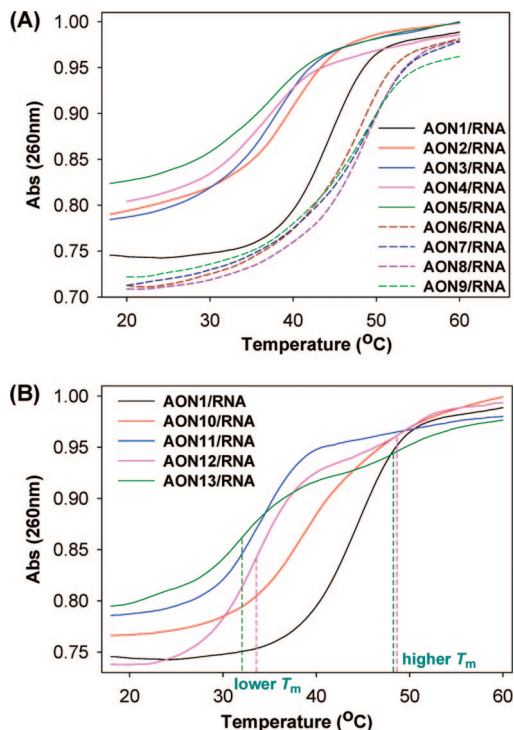


FIGURE 10. Melting curves of duplexes formed by AONs 1–9 with complementary RNA (panel A) and AONs 10–13 with complementary RNA (panel B). The samples of AON 10, AON 12, and AON 13 were contaminated with about 20% of AON 6, AON 8, and AON 9, respectively, so in their melting curves especially for AON 12 and AON 13, two transitions can be observed (panel B). The first transition (lower T_m) corresponds to the dissociation of AON 12 (pink) or AON 13 (dark green) form RNA, and the second transition (higher T_m) corresponds to dissociation of the impurities AON 8 (pink) or AON 9 (dark green) form RNA.

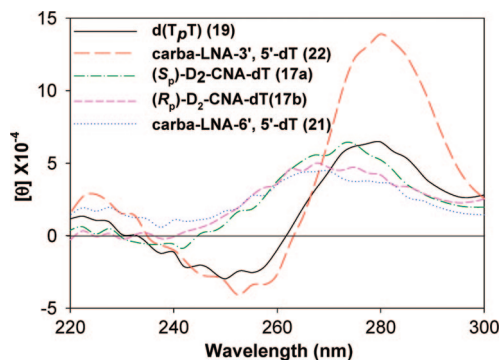


FIGURE 11. Circular dichroic spectra of (S_p)-D₂-CNA-dT dimer 17a, dTpdT (19), carba-LNA-3',5'-dT dimer (22), and carba-LNA-6',5'-dT dimer (21) in 60 mM Tris-HCl (pH 7.5), 60 mM KCl, 0.8 mM MgCl₂ at 5 °C. Dimer concentration, 0.1 mM.

dinucleotide level the rotational strength of the CD spectrum at 260–280 nm is proportional to the base–base overlap.^{54,73} Here, CD spectra of native dimers d(T_pT) (19), (S_p)-D₂-CNA-dT (17a), carba-LNA-3',5'-dT (22), and carba-LNA-6',5'-dT (21) were recorded and are shown in Figure 11. The maximum and minimum positions of the magnitude of the molecular ellipticities (θ) is very similar for (S_p)-D₂-CNA-dT (17a), (R_p)-D₂-CNA-dT (17b), and carba-LNA-6',5'-dT (21), and they all show minima at 238 nm and maxima at 275 nm. In contrast, the maximum (at 254 nm) and minimum (at 280 nm) positions of the molecular ellipticities are very similar for carba-LNA-3',5'-dT (22) and d(T_pT) (19), but the magnitude of the molecular

ellipticities at 280 nm for d(T_pT) (19) is almost ~60% less than that of carba-LNA-3',5'-dT (22). This shows that carba-LNA-3',5'-dT (22) has more increased rotational strength vis-à-vis d(T_pT) (19), which is consistent with an enhanced interaction between the electric dipoles of the adjacent thymine base, resulting from more base–base overlap) in carba-LNA-3',5'-dT (22) than that of dTpdT (19), as well as in comparison with those of (S_p)-D₂-CNA-dT (17a), (R_p)-D₂-CNA-dT (17b), and carba-LNA-6',5'-dT (21). At 270–280 nm, the magnitude of the molecular ellipticities follow this sequence: carba-LNA-3',5'-dT (22) \gg d(T_pT) (19) > (S_p)-D₂-CNA-dT (17a) > (R_p)-D₂-CNA-dT (17b) > carba-LNA-6',5'-dT (21), suggesting that base–base stacking in these dimers also follow this ranking. Therefore, (S_p)-D₂-CNA in AONs 2–5 and carba-LNA-6',5'-phosphodiester modification in AONs 10–13 make a stacking geometry distortion in AON/RNA and AON/DNA duplexes, and it is likely that they can not be base-paired with the complementary nucleobases in the opposite strand. This conclusion is consistent with the thermal denaturation studies in that in this 15mer AON/RNA duplex, a single mismatch leads to T_m decrease about -9 to -12 °C⁷⁴ and T_m decrease in this AON/RNA duplex induced by single (S_p)-D₂-CAN modification (about -7 °C) or especially carba-LNA-6',5'-phosphodiester modification (-10 to -12 °C) exactly fall in this range.

Conclusions

(1) Two diastereoisomers of (S_p or R_p)-D₂-CNA -dT dimers have been constructed by coupling the cis-orientated 3'-OH and 6'-OH of the carba-LNA nucleoside with 5'-thymidine phosphoramidite to form a rigid tricyclic phosphotriester system in which not only the sugar pucker (ν_0 – ν_4) but the phosphate backbone torsions δ, ϵ, ζ are conformationally constrained. The formation of this unique tricyclic system was confirmed by ¹H, ¹H{³¹P}, ¹³C, ³¹P, ¹H, ³¹P-COSY, HMQC, HMBC, and 1D and 2D NOESY NMR experiments.

(2) The structures of D₂-CNA were established on the basis of NMR as well as ab initio calculations. Compared to native DNA and other δ, ϵ, ζ -constrained CNAs, the D₂-CNAs have two unique structural features: first, the sugar is locked in extreme N-type with $P = 11^\circ$ and $\Phi_m = 54^\circ$; second, the fixed backbone torsions δ, ϵ, ζ were determined by δ (g⁺), ϵ (cis), ζ (a⁺) for (S_p) D₂-CNA and δ (g⁺), ϵ (cis), ζ (a⁻) for (R_p) D₂-CNA. To the best of our knowledge, the diastereomerically pure D₂-CNAs are the first reported molecules that have the unique locked cis conformation across the backbone torsion ϵ .

(3) The dioxaphosphorinane ring in D₂-CNA was chemically unstable under standard deprotection conditions using aqueous ammonia: Thus, in 1M NaOH solution, the phosphotriester in D₂-CNA was 200 times more unstable than unconstrained methyl phosphotriester. In concentrated aqueous ammonia, $t_{1/2}$ were 12 and 6 min for (S_p)- and (R_p)-D₂-CNA, respectively. But D₂-CNA was very stable toward weak nucleophile such as hydrazine hydrate in pyridine/AcOH, and it was also stable toward non-nucleophilic strong base such as DBU in MeCN.

(4) D₂-CNA was found to be resistant toward nuclease digestion.

(5) F⁻-catalyzed isomerization of (S_p)-D₂-CNA \rightleftharpoons (R_p)-D₂-CNA and its dynamic equilibrium have been studied by NMR. The (S_p)-D₂-CNA was 0.39 kcal/mol more stable than that of the (R_p)-isomer. A possible mechanism for this unusual isomer-

(74) Zhou, C.; Chattopadhyaya, J. *ARKIVOC* 2009, (iii), 171–186.

ization has been proposed in light of all experimental facts underlying the cleavage reaction of pure (S_p)-D₂-CNA and (R_p)-D₂-CNA. We have argued for a pseudorotational pathway to explain the observed character of the dynamic equilibrium of the (S_p)-D₂-CNA \rightleftharpoons (R_p)-D₂-CNA isomerization process. This work therefore shows that the pseudorotation of phosphorus trigonal-bipyramidal intermediate is still possible in the conformational equilibrium of the highly constrained systems.

(6) The (S_p)-D₂-CNA has been incorporated into antisense oligodeoxynucleotides (AON) basing on the solid supported DNA synthesis strategy. A new strategy has been developed to deprotect D₂-CNA modified AONs. Thus, DBU/MeCN have been successfully used to cleave the modified oligos from the solid support, and hydrazine hydrate in pyridine/AcOH has been subsequently used to deprotect the nucleobase protecting groups (PAC), under which D₂-CNA was satisfactorily stable. The intact nature of the internucleotidic phosphotriester (as in (S_p)-D₂-CNA) function in the modified AONs have been unequivocally evidenced by Maldi-Tof mass measurements.

(7) Treatment of (S_p)-D₂-CNA modified AON with concentrated aqueous ammonia gave carba-LNA-6',5'-phosphodiester modified AON plus small amount (about 20%) of carba-LNA-3',5'-phosphodiester modified AON, which agrees well with our detailed study on the modified dimers.

(8) Thermal denaturation studies have shown that carba-LNA-3',5'-phosphodiester modification stabilized AON/RNA duplex by +4 °C/modification. (S_p)-D₂-CNA modification destabilized AON/RNA duplex by about -7 °C/modification and carba-LNA-6',5'-phosphodiester modification even exert a much more negative effect on the AON/RNA thermal stability (-10 to -12 °C/modification). CD spectroscopy studies in the dinucleotides level suggested the base stacking in these three modifications follow this rank: carba-LNA-3',5'-dT \gg native d(T_pT) > (S_p)-D₂-CNA-dT > carba-LNA-6',5'-dT, which coincide with the rank of their effect on the thermal stability, thus formation of C6'-OP bond in carba-LNA indeed make a geometry distortion in the AON/RNA and AON/DNA duplexes.

Experimental Section

(1R,3R,4R,5S,6S,7S)-7-(Benzyloxy)-1-((benzyloxy)methyl)-5-methyl-6-tosylate-3-(thymine-1-yl)-2-oxabicyclo[2.2.1]heptane (2). Compound **1** (1.26 g, 2.6 mmol) was coevaporated with dry pyridine twice and dissolved in the same solvent, to which was added 4-methylbenzoyl chloride (0.61 g, 3.2 mmol). The reaction mixture was stirred at room temperature for 12 h. Then another part of 4-methylbenzoyl chloride (0.61 g, 3.2 mmol) was added and the mixture stirred for a further 24 h. Pyridine was recovered under reduced pressure, and the residue was diluted with CH₂Cl₂ and washed with saturated NaHCO₃ solution. The organic layer was dried with MgSO₄ and concentrated under reduced pressure to give crude product, which was subjected to short column chromatography on silica gel (10–40% ethyl acetate in cyclohexane, v/v) to give **2** (1.57 g, 94%) as white foam. ¹H NMR (500 MHz, CDCl₃): δ 8.42 (broad, H3), 7.78 (d, $J = 8.5$ Hz, 2H, aromatic), 7.64 (s, 1H, H6), 7.34–7.21 (m, 12H), 5.71 (s, 1H, H1'), 4.98 (d, $J_{6,7} = 9.5$ Hz, 1H, H6'), 4.54–4.41 (m, 4H, BnCH₂), 4.04 (s, 1H, H3'), 3.70 (d, $J_{gem} = 11.0$ Hz, H5'), 3.59 (d, $J_{gem} = 11.0$ Hz, H5''), 2.83 (m, 1H, H7'), 2.63 (d, $J_{2,7} = 3.5$ Hz, 1H, H2'), 2.46 (s, 3H, Tol-CH₃), 1.46 (s, 3H, T-CH₃), 1.07 (d, $J_{7,7Me} = 7.5$ Hz, 3H, 7'-Me). ¹³C NMR (150 MHz, CDCl₃): δ 163.7 (C4), 149.6 (C2), 145.2, 137.5, 136.7, 135.9, 133.4, 129.9, 128.6, 128.3, 128.1, 127.9, 127.8, 127.7, 109.5 (C5), 87.9 (C4'), 83.6 (C1'), 79.9 (C6'), 77.3 (C3'), 73.8, 72.4 (Bn-CH₂), 65.5 (C5'), 47.8 (C2'), 32.5 (C7'), 21.7 (Tol-Me), 11.9 (T-Me), 9.2 (7'-Me). MALDI-TOF m/z : [M + H]⁺ found 633.6, calcd 633.2.

(1R,3R,4R,5S,6S,7S)-1-(4,4'-Dimethoxytrityloxymethyl)-7-hydroxy-5-methyl-6-tosylate-3-(thymine-1-yl)-2-oxabicyclo[2.2.1]heptane (4). To a solution of compound **2** (1.5 g, 2.37 mmol) in dry methanol (20 mL) were added 20% Pd(OH)₂/C (1.15 g) and ammonium formate (2.9 g, 46 mmol) and the mixture refluxed for 2 h. Then another part of 20% Pd(OH)₂/C (1.15 g) and ammonium formate (2.9 g) was added and the mixture refluxed for an additional 2 h. Then, 1.15 g of 20% Pd(OH)₂/C and 2.9 g of ammonium formate were added again and the mixture heated under reflux for a further period of 3 h. The suspension was filtered over a Celite bar, and the organic phase was evaporated to dryness. The residue was coevaporated twice with dry pyridine and dissolved in the same solvent. 4,4'-Dimethoxytrityl chloride (0.8 g) was added and stirred overnight at room temperature. Then the solvent was removed and residue was diluted with CH₂Cl₂, washed with saturated NaHCO₃ solution, dried over MgSO₄, and subjected to chromatography on silica gel (methanol in dichloromethane containing 1% pyridine, 0.5–1.5%, v/v) to give **4** (1.32 g, 74%). ¹H NMR (500 MHz, CDCl₃): δ 8.49 (broad, 1H, H3), 7.72 (s, 1H, H6), 7.64 (d, $J = 8.0$ Hz, 2H, aromatic), 7.33–6.81 (m, 15H), 5.71 (s, 1H, H1'), 4.83 (d, $J_{6,7} = 9.5$ Hz, 1H, H6'), 4.30 (s, 1H, H3'), 3.80 (two singlet, 6H, OMe), 3.41 (d, $J_{gem} = 11.0$ Hz, H5'), 3.11 (d, $J_{gem} = 11.0$ Hz, H5''), 2.93 (m, 1H, H7'), 2.58 (d, $J_{2,7} = 1.5$ Hz, 1H, H2'), 2.38 (s, 3H, Tol-Me), 2.29 (broad, 1H, 3'-OH), 1.51 (s, 3H, T-Me), 1.14 (d, $J_{7,7Me} = 7.5$ Hz, 3H, 7'-Me). ¹³C NMR (150 MHz, CDCl₃): δ 163.9 (C4), 158.8, 158.7, 149.7 (C2), 144.8, 144.1, 136.1, 135.2, 135.1, 133.5, 130.1, 130.0, 129.7, 128.1, 128.0, 127.8, 127.2, 113.3, 113.2, 109.8 (C5), 88.4 (C4'), 86.9 (DMTr), 83.6 (C1'), 80.7 (C6'), 71.7 (C3'), 58.6 (C5'), 55.3 (OMe), 50.1 (C2'), 32.3 (C7'), 21.6 (Tol-Me), 12.3 (T-Me), 9.1 (7'-Me). MALDI-TOF m/z : [M + Na]⁺ found 777.3, calcd 777.3.

(1R,3R,4R,5S,6S,7S)-1-(4,4'-Dimethoxytrityloxymethyl)-7-(cyanoethyl 5'-O-(3'-O-tert-butylidimethylsilyl)thymidinyl phosphate)-5-methyl-6-tosylate-3-(thymine-1-yl)-2-oxabicyclo[2.2.1]heptane (6). Compound **4** (0.6 g, 0.79 mmol) was dissolved in dry MeCN, to which were added 5-ethylthio-1H-tetrazole (0.67 g, 8 mmol) and 5'-phosphoramidite-3'-tert-butylidimethylsilyl thymidine (0.58 g, 1 mmol). After being stirred at rt for 4 h, 0.1 M I₂ in THF–H₂O–pyridine (7:1:2) (20 mL) was added and stirred at rt for 1 h. Then the solvent was evaporated under reduced pressure, and the residue was dissolved in ethyl acetate, washed with aqueous Na₂S₂O₃ solution (15%, 100 mL) twice, and then saturated NaHCO₃ and brine successively, and dried over MgSO₄. The mixture was then concentrated under reduced pressure to give crude product, which was subjected to short column chromatography on silica gel (acetone in dichloromethane containing 2% pyridine, 5–25% v/v) to give **6** (1.1 g, 89%) as a mixture of two diastereoisomers. ³¹P NMR (202.5 MHz, CDCl₃): δ -0.59, -1.28. ¹H NMR (500 MHz, CDCl₃): δ 7.66 (1H, s, H6), 7.67 (1H, s, H6), 7.60 (2H, d, $J = 8.3$ Hz, Ts-aromatic), 7.56 (2H, d, $J = 8.3$ Hz, Ts-aromatic), 7.33–7.05 (22H, m, aromatic), 6.82 (8H, m, DMTr-aromatic), 6.16 (1H, t, $J = 6.4$ Hz, H1'b), 6.13 (1H, t, $J = 6.4$ Hz, H1'b), 5.76 (1H, s, H1'a), 5.74 (1H, s, H1'a), 5.07 (1H, dd, $J_{H3'a,P} = 6.1$ Hz, $J_{H3'a,H2'a} = 1.9$ Hz, H3'a), 5.06 (1H, dd, $J_{H3'a,P} = 6.0$ Hz, $J_{H3'a,H2'a} = 1.9$ Hz, H3'a), 4.80 (1H, d, $J_{H6'a,H7'a} = 9.4$ Hz, H6'a), 4.66 (1H, d, $J_{H6'a,H7'a} = 9.4$ Hz, H6'a), 4.31 (m, 2H, two H3'b), 4.22–4.15 (4H, m, two H5'b, POCH₂CH₂CN), 3.92 (2H, m, H5'b, H4'b), 3.88 (1H, m, POCH₂CH₂CN), 3.81–3.79 (four singlet, 12H, four OMe), 3.66 (1H, m, H5''b), 3.58 (1H, m, POCH₂CH₂CN), 3.52 (m, 1H, H4''b), 3.39 (1H, d, $J_{gem} = 11.3$ Hz, H5'a), 3.29 (1H, d, $J_{gem} = 11.3$ Hz, H5'a), 3.06 (1H, d, $J_{gem} = 11.3$ Hz, H5''a), 3.03 (1H, d, $J_{gem} = 11.3$ Hz, H5''a), 2.89 (2H, m, two H2'a), 2.85 (m, 1H, H7'a), 2.78 (m, 1H, H7'a), 2.45 (1H, m, POCH₂CH₂CN), 2.40 (3H, s, Ts-Me), 2.39 (3H, s, Ts-Me), 2.27–2.21 (5H, m, two H2'b, two H2''b, POCH₂CH₂CN), 1.90 (3H, s, T-Me), 1.89 (3H, s, T-Me), 1.25 (6H, s, T-Me), 1.19 (3H, d, $J = 7.6$ Hz, 7'-Me), 1.16 (3H, d, $J = 7.6$ Hz, 7'-Me), 0.88 (18H, s, Si(CH₃)₃), 0.80–0.06 (12H, four singlet, (Si(CH₃)₂)). ¹³C NMR (125 MHz, CDCl₃): δ 163.8, 164.3, 164.2, 164.1, 163.9, 150.2, 149.9, 159.31, 159.28, 150.65, 150.52,

150.38, 150.37, 145.40, 145.38, 143.88, 136.15, 136.03, 135.20, 135.14, 135.09, 135.04, 134.90, 133.82, 133.71, 130.79, 130.77, 130.70, 130.64, 130.14, 130.12, 128.99, 128.94, 128.45, 128.41, 128.16, 128.06, 127.90, 116.57, 116.49, 113.66, 113.63, 113.60, 111.77, 111.68, 111.05, 88.42 (d, $J_{C4'a,P} = 4.6$ Hz, C4'a), 88.37 (d, $J_{C4'a,P} = 4.6$ Hz, C4'a), 87.51, 87.48, 86.6 (C1'b), 85.6 (C1'b), 84.9 (d, $J_{C4'b,P} = 6.5$ Hz, C4'b), 84.6 (d, $J_{C4'b,P} = 6.5$ Hz, C4'b), 83.7 (C1'a), 83.6 (C1'a), 79.78 (C6'a), 79.77 (C6'a), 76.94 (d, $J_{C3'a,P} = 4.6$ Hz, C3'a), 76.92 (d, $J_{C3'a,P} = 4.6$ Hz, C3'a), 71.4 (C3'b), 70.4 (C3'b), 67.9 (d, $J_{C,P} = 6.5$ Hz, OCH₂CH₂CN), 66.6 (d, $J = 5.5$ Hz, OCH₂CH₂CN), 63.1 (d, $J_{C5'b,P} = 4.6$ Hz, C5'b), 62.6 (d, $J_{C5'b,P} = 4.6$ Hz, C5'b), 58.5 (C5'a), 58.3 (C5'a), 55.73(OMe), 55.67 (OMe), 49.5 (two C2'a), 40.3, 40.8 (C2'b), 40.6(C2'b), 26.1 (Si(C(CH₃)₃)), 22.12(Ts-Me), 22.10 (Ts-Me), 20.10 (d, $J_{C,P} = 6.5$ Hz, OCH₂CH₂CN), 19.81 (d, $J_{C,P} = 7.4$ Hz, OCH₂CH₂CN), 18.28, 18.26, 12.92, 12.71, 12.59, 12.57 (T-Me), 9.23(7'-Me), 9.21 (7'-Me), -4.28, -4.30, -4.51, -4.57 (Si (CH₃)₂). MALDI-TOF *m/z*: [M + K]⁺ found 1264.38, calcd 1264.381.

(1R,3R,4R,5S,6R,7S)-7-(Benzyloxy)-1-((benzyloxy)methyl)-5-methyl-6-acetate-3-(thymine-1-yl)-2-oxabicyclo[2.2.1]heptane (10). Compound **1** (100 mg, 0.21 mmol) was coevaporated with dry pyridine twice and dissolved in dry DCM (4 mL) containing 0.12 mL of dry pyridine, cooled to -10 °C. Triflic anhydride (55 μL, 0.31 mmol) in 1 mL of dry CH₂Cl₂ was added dropwise under N₂. The reaction mixture was kept at -10 °C for 10 min and then allowed to warm to rt over 1 h followed by pouring into ice-cooled saturated NaHCO₃ solution. The solution was extracted with CH₂Cl₂ twice, and the organic phase was dried over MgSO₄. Evaporation of solvent under vacuum give crude product **9**. The crude product was dissolved in 3 mL of dry DMF, to which were added CsOAc (120 mg, 0.63 mmol) and 18-crown-6 (55 mg, 0.21 mmol). The reaction mixture was stirred at rt overnight and then at 60 °C for 24 h. A small amount of the major product (less than 20% from TLC) was separated by short column chromatography on silica gel (20–40% ethyl acetate in cyclohexane, v/v), and NMR characterization proved it to be the desired product **10**. ¹H NMR (600 MHz, CDCl₃): δ 8.73 (broad, H3), 7.66 (s, 1H, H6), 7.35–7.26 (m, 10H), 5.65 (s, 1H, H1'), 4.60–4.49 (m, 5H, BnCH₂, H6'), 4.12 (s, 1H, H3'), 3.92 (d, $J_{gem} = 11.4$ Hz, H5'), 3.82 (d, $J_{gem} = 11.4$ Hz, H5''), 2.71 (d, $J_{2,7'} = 3.6$ Hz, 1H, H2'), 2.61 (m, 1H, H7'), 2.07 (s, 3H, COCH₃), 1.50 (s, 3H, T-CH₃), 1.38 (d, $J_{7,7'Me} = 7.8$ Hz, 3H, 7'-Me). ¹³C NMR (150 MHz, CDCl₃) δ: 170.5 (C=O), 163.9 (C4), 149.8 (C2), 137.6, 137.5, 136.0, 128.6, 128.4, 128.1, 127.9, 127.8, 127.2, 109.5 (C5), 87.6 (C4'), 83.5(C1'), 80.2(C6'), 78.1 (C3'), 73.9, 71.7 (Bn-CH₂), 65.7 (C5'), 48.2 (C2'), 38.7 (C7'), 20.9 (CH₃C=O), 13.4 (7'-Me), 12.0 (T-Me), MALDI-TOF M/S: [M + H]⁺ found 521.23, calcd 521.247.

(1R,3R,4R,5S,6R,7S)-7-Benzyloxy-1-benzyloxymethyl-6-hydroxyl-3-(thymine-1-yl)-2-oxabicyclo[2.2.1] heptane (11). Compound **1** (551 mg, 1.15 mmol) was dissolved in dry CH₂Cl₂ (3 mL), and 15% Dess–Martin periodinane in CH₂Cl₂ (3.2 mL, 1.5 mmol) was added dropwise under nitrogen. After being stirred at room temperature for 2 h, the reaction mixture was diluted with CH₂Cl₂ and filtered through a Celite bar. The filtrate was washed with saturated Na₂S₂O₃ solution and NaHCO₃ successively and dried over MgSO₄. After evaporation of solvent under reduced pressure ketone **12** was obtained quantitatively. ¹H NMR (600 MHz, CDCl₃): δ 8.72 (broad, H3), 7.70 (s, 1H, H6), 7.35–7.19 (m, 10H), 5.76 (s, 1H, H1'), 4.64–4.49 (m, 4H, BnCH₂), 4.26 (s, 1H, H3'), 4.00 (d, $J_{gem} = 11.5$ Hz, H5'), 3.85 (d, $J_{gem} = 11.5$ Hz, H5''), 3.08 (m, 1H, H2'), 2.86 (m, 1H, H7'), 1.54 (s, 3H, T-CH₃), 1.33 (d, $J_{7,7'Me} = 7.5$ Hz, 3H, 7'-Me). ¹³C NMR (150 MHz, CDCl₃) δ: 206.6 (C=O), 163.8 (C4), 149.8 (C2), 137.3, 136.4, 135.7, 128.7, 128.6, 128.3, 128.2, 127.9, 127.6, 109.9 (C5), 86.3 (C4'), 84.0(C1'), 75.7 (C3'), 74.1, 72.3 (Bn-CH₂), 63.2 (C5'), 46.4 (C2'), 40.3 (C7'), 12.1 (T-Me), 9.5 (7'-Me). MALDI-TOF M/S: [M + H]⁺ found 477.2, calcd 477.2. The crude ketone was dissolved in 95% ethanol, and NaBH₄ (47 mg, 1.24 mmol) was added in portions. The mixture was allowed to stir at room temperature for 2 h. Then solvent was removed, and the

residue was extracted with CH₂Cl₂. The organic layer was washed with saturated NaHCO₃, dried over MgSO₄, and evaporated to give crude product, which was subjected to short column chromatography on silica gel (ethyl acetate in cyclohexane, 20–60% v/v) to give **11** (297 mg, 54%) and 219 mg of substrate **1** (40%). **11**. ¹H NMR (600 MHz, CDCl₃): δ 8.75 (broad, H3), 7.72 (s, 1H, H6), 7.36–7.22 (m, 10H), 5.59 (s, 1H, H1'), 4.65–4.44 (m, 4H, BnCH₂), 4.17 (s, 1H, H3'), 4.04 (d, $J_{gem} = 11.5$ Hz, H5'), 3.96 (d, $J_{gem} = 11.5$ Hz, H5''), 3.32 (ddd, $^3J_{6'H,6'OH} = 12.3$ Hz, $^WJ_{6'H,3'H} = 1.9$ Hz, $^3J_{6'H,7'H} = 3.4$ Hz, 1H, H6'), 2.82 (d, $^3J_{2'H,7'H} = 3.5$ Hz, 1H, H6'), 2.46 (d, $^3J_{6'H,6'OH} = 12.3$ Hz, 1H, 6'OH), 2.31 (m, 1H, H7'), 1.52 (s, 3H, T-CH₃), 1.36 (d, $J_{7,7'Me} = 7.5$ Hz, 3H, 7'-Me). ¹³C NMR (150 MHz, CDCl₃): δ 163.9 (C4), 149.9 (C2), 137.6, 136.3, 136.1, 128.7, 128.6, 128.5, 128.1, 128.0, 127.9, 109.5 (C5), 86.9 (C4'), 83.7(C1'), 81.0 (C6'), 79.5 (C3'), 73.9, 72.5 (Bn-CH₂), 65.7 (C5'), 47.2 (C2'), 42.2 (C7'), 13.4 (7'-Me), 12.1 (T-Me). MALDI-TOF *m/z*: [M + H]⁺ found 479.217, calcd 479.218.

(1R,3R,4R,5S,6S,7S)-1-(4,4'-Dimethoxytrityloxymethyl)-7-hydroxyl-5-methyl-6-tosylate-3-(thymine-1-yl)-2-oxabicyclo[2.2.1] heptane (13). To a solution of compound **11** (440 mg, 0.92 mmol) in dry methanol (10 mL) were added 20% Pd(OH)₂/C (0.92 g) and ammonium formate (2.32 g, 36.8 mmol) and the mixture refluxed for 2 h. The suspension was filtered over a Celite bar, and the organic phase was evaporated to dryness. The residue was co-evaporated with dry pyridine twice and dissolved in the same solvent. 4,4'-Dimethoxytrityl chloride (320 mg, 0.94 mmol) was added and the mixture stirred overnight at room temperature. Then the solvent was removed and residue was diluted with CH₂Cl₂, washed with saturated NaHCO₃ solution, dried over MgSO₄, and subjected to chromatography on silica gel (methanol in dichloromethane containing 1% pyridine, 1–3%, v/v) to give product **13** (424 mg, 77%). ¹H NMR (500 MHz, CDCl₃): δ 8.76 (broad, 1H, H3), 7.76 (s, 1H, H6), 7.47–6.83 (m, 13H), 5.56 (s, 1H, H1'), 4.43 (s, 1H, H6'), 3.78 (m, 7H, OMe, H5'), 3.73 (d, $J_{gem} = 11.5$ Hz, H5''), 3.35 (s, 1H, H3'), 2.71 (d, $J_{2,7'} = 4.0$ Hz, 1H, H2'), 2.43 (m, 1H, H7'), 1.52 (s, 3H, T-Me), 1.34 (d, $J_{7,7'Me} = 7.0$ Hz, 3H, 7'-Me). ¹³C NMR (150 MHz, CDCl₃): δ 164.0 (C4), 158.7, 149.8 (C2), 144.5, 135.8, 135.7, 135.6, 130.1, 130.0, 128.2, 128.1, 127.1, 113.3, 113.2, 109.7 (C5), 87.4 (C4'), 86.9 (DMTr), 83.9 (C1'), 80.7 (C6'), 73.8 (C3'), 59.3 (C5'), 55.3 (OMe), 49.8 (C2'), 29.7 (C7'), 13.4 (7'-Me), 12.3 (T-Me). MALDI-TOF *m/z*: [M + Na]⁺ found 623.2, calcd 623.2.

5'-a-O-Dimethoxytrityl-3'-b-O-tert-butylidimethylsilyl-(S_p)-D₂-CNA-dT (15a) and 5'-a-O-Dimethoxytrityl-3'-b-O-tert-butylidimethylsilyl-(R_p)-D₂-CNA-dT (15b). 3'-O-tert-Butylidimethylsilylthymidine (374 mg, 1.05 mmol) was coevaporated with dry toluene twice and dissolved in dry CH₂Cl₂. Triethylamine (0.22 mL, 1.58 mmol) was added followed by bis(diisopropylamine) chlorophosphoramidite (370 mg, 1.16 mmol). After reaction at rt for 1 h, filtration through dry cotton, and evaporation gave crude 3'-O-tert-butylidimethylsilyl thymidine-5'-O-phosphordiamidite **14**. The crude compound **14** was dissolved in 5 mL of dry MeCN, to which was added 5-ethylthio-1H-tetrazole (364 mg, 2.8 mmol) followed by compound **13** (420 mg, 0.7 mmol). After reaction at rt for 2 h, 0.1 M I₂ in THF–H₂O–pyridine (7:1:2) (20 mL) was added and the mixture stirred at rt for further 1 h. Then the reaction mixture was diluted with EtOAc and washed with aqueous Na₂S₂O₃ solution (15%, 100 mL) twice, saturated NaHCO₃ once, and brine once successively and dried over MgSO₄. Then concentration under reduced pressure gave crude product, which was subjected to short column chromatography on silica gel (acetone in petroleum ether containing 1% pyridine, 20–55% v/v) to give **15a** (271 mg, 38.7%) and **15b** (113 mg, 16.1%). **15a**. ³¹P NMR (202.5 MHz, CDCl₃): δ -8.1. ¹H NMR (500 MHz, CDCl₃): δ 9.25 (broad, 1H, H3), 9.12 (broad, 1H, H3), 7.65 (s, 1H, H6), 7.55–6.84 (m, 15H), 6.23 (dd, $J_{H1'b,H2'b} = 4.9$ Hz, $J_{H1'b,H2'b} = 6.0$ Hz, 1H, H1'b), 5.52 (s, 1H, H1'a), 5.07 (d, $J_{H3'a,p} = 16.6$ Hz, 1H, H3'a), 4.37–4.28 (m, 3H, H5'b, H5'c, H3'b), 4.18 (d, $J_{gem} = 12.1$ Hz, 1H, H5'a), 4.05 (m, 1H, H4'b), 3.96 (d, $J_{H6'a,p} = 24.6$ Hz, 1H, H6'a), 3.80 (m, 6H, OMe),

3.74 (d, $J_{gem} = 12.1$ Hz, 1H, H5''a), 3.23 (d, $J_{H2'a,H7'a} = 4.9$ Hz, 1H, H2'a), 3.04 (m, 1H, H7'a), 2.32 (m, 1H, H2'b), 2.07 (m, 1H, H2''b), 1.89 (s, 3H, T-Me), 1.34 (d, $J_{H7'a,7'Me} = 7.6$ Hz, 3H, 7'-Me), 1.30 (s, 3H, T-Me), 0.90 (s, 9H, *tert*-butyl), 0.12 (s, 6H). ^{13}C NMR (125 MHz, $CDCl_3$): δ 163.9(C4), 163.8 (C4), 158.8, 158.7, 150.2 (C2), 145.0 (C2), 143.9, 135.4, 135.1, 134.7, 134.6, 130.1, 130.0, 128.2, 128.1, 127.3, 113.5, 113.4, 111.1 (C5), 110.8 (C5), 87.4, 85.6 (C1'b), 85.1 (d, $J = 6.4$ Hz, C4'b), 83.9 (d, $J = 6.4$ Hz, C6'a), 83.7(d, $J = 7.3$ Hz, C4'a), 83.4(C1'a), 81.2 (d, $J = 9.2$ Hz, C3'a), 71.6 (C3'b), 67.9 (d, $J = 4.4$ Hz, C5'b), 58.4 (C5'a), 55.2 (OMe), 49.2 (C2'a), 40.6 (C2'b), 37.9 (C7'a), 25.7 (tBDMS), 17.9 (tBDMS), 13.4 (7'-Me), 12.5 (T-Me), 11.9 (T-Me), -4.7(tBDMS), -4.8 (tBDMS). MALDI-TOF M/S: $[M + Na]^+$ found 1023.36, calcd 1023.36. **15b**. ^{31}P NMR (202.5 MHz, $CDCl_3$): δ -7.1. 1H NMR (500 MHz, $CDCl_3$): δ 9.01 (broad, 1H, H3), 8.82 (broad, 1H, H3), 7.85 (s, 1H, H6), 7.45-6.83 (m, 15H), 6.25 (dd, $J_{H1'b,H2'b} = 5.8$ Hz, $J_{H1'b,H2''b} = 7.6$ Hz, 1H, H1'b), 5.61 (s, 1H, H1'a), 5.07 (d, $J_{H3'a,p} = 17.9$ Hz, 1H, H3'a), 4.28 (m, 1H, H3'b), 4.02-3.78 (m, 11H, H5'b, H6'a, H5''b, H5'a, H5''a, H4'b, OMe), 3.29 (m, 1H, H7'a), 3.24 (d, $J_{H2'a,H7'a} = 5$ Hz, 1H, H2'a), 2.24 (m, 1H, H2'b), 2.00 (m, 1H, H2''b), 1.88 (s, 3H, T-Me), 1.43 (d, $J_{H7'a,7'Me} = 7.5$ Hz, 3H, 7'-Me), 1.22(s, 3H, T-Me), 0.90 (s, 9H, *tert*-butyl), 0.12 (s, 6H). ^{13}C NMR (125 MHz, $CDCl_3$): δ 163.7(C4), 163.6 (C4), 158.9, 150.2 (C2), 149.8 (C2), 143.7, 135.6, 134.8, 134.7, 134.6, 130.3, 130.2, 128.3, 128.1, 127.5, 113.4, 113.3, 111.1 (C5), 110.8 (C5), 87.4, 85.2 (C1'b), 84.9 (d, $J = 4.6$ Hz, C4'b), 83.9 (d, $J = 5.5$ Hz, C6'a), 83.4 (C1'a), 83.2 (d, $J = 5.5$ Hz, C4'a), 81.2 (d, $J = 10.1$ Hz, C3'a), 71.8 (C3'b), 67.9 (d, $J = 5.5$ Hz, C5'b), 58.6 (C5'a), 55.3 (OMe), 49.3 (C2'a), 40.4 (C2'b), 39.0 (C7'a), 25.7 (tBDMS), 17.9 (tBDMS), 13.4 (7'-Me), 12.3 (T-Me), 11.7 (T-Me), -4.7(tBDMS), -4.8 (tBDMS). MALDI-TOF M/S: $[M + Na]^+$ found 1023.36, calcd 1023.366.

5'a-O-Dimethoxytrityl-(S_p)-D₂-CNA-dT (16a) and 5'a-O-Dimethoxytrityl-(R_p)-D₂-CNA-dT (16b). **15a** (150 mg, 0.15 mmol) was dissolved in 3 mL dry THF, to which 0.25 mL of 1 M TBAF/THF was added. The mixture was allowed to stir at room temperature for 20 min. After evaporation of solvent on vacuum, the residue was subjected to short column chromatography on silica gel (EtOAc/MeCN = 7/3 containing 1% pyridine, methanol from 1% to 3%) to give **16a** (99 mg, 74.5%) and **16b** (19 mg, 14.3%). **16a** and **16b** can also be obtained from **15b**, thus **15b** (60 mg, 0.06 mmol) was dissolved in 2 mL dry THF, to which 0.12 mL of 1 M TBAF/THF was added. The mixture was allowed to stir at room temperature for 20 min. After evaporation of solvent on vacuum, the residue was subjected to short column chromatography on silica gel (EtOAc/MeCN = 7/3 containing 1% pyridine, methanol from 1% to 3%) to give **16a** (17 mg, 32%) and **16b** (31 mg, 58%). **16a**. ^{31}P NMR (202.5 MHz, $CDCl_3$): δ -6.5. 1H NMR (500 MHz, $CDCl_3$): δ 7.59 (s, 1H, H6), 7.45-6.84 (m, 14H), 6.24 (t, $J = 5.5$ Hz, 1H, H1'b), 5.50 (s, 1H, H1'a), 5.05 (d, $J_{H3'a,p} = 17.0$ Hz, 1H, H3'a), 4.45 (m, 1H, H3'b), 4.37 (dd, $J_{H5'b,H4'b} = 3.4$ Hz, $J_{H5'b,p} = 9.0$ Hz, 2H, H5'b, H5''b), 4.10 (m, 2H, H5'a, H4'b), 3.98 (d, $J_{H6'a,p} = 24.9$ Hz, 1H, H6'a), 3.78 (s, 6H, OMe), 3.74 (d, $J_{gem} = 12.1$ Hz, 1H, H5''a), 3.26 (d, $J_{H2'a,H7'a} = 4.9$ Hz, 1H, H2'a), 3.05 (m, 1H, H7'a), 2.44 (m, 1H, H2'b), 2.12 (m, 1H, H2''b), 1.88 (s, 3H, T-Me), 1.32 (d, $J_{H7'a,7'Me} = 7.2$ Hz, 3H, 7'-Me), 1.30 (s, 3H, T-Me). ^{13}C NMR (125.0 MHz, $CDCl_3$): δ 163.9(C4), 158.8, 158.7, 150.5 (C2), 150.2 (C2), 143.9, 135.5, 135.1, 134.8, 134.6, 130.1, 128.2, 128.1, 127.3, 113.5, 111.2 (C5), 110.9 (C5), 87.5, 85.4 (C1'b), 84.6 (d, $J = 5.5$ Hz, C4'b), 84.1 (d, $J = 4.6$ Hz, C6'a), 83.7(d, $J = 7.3$ Hz, C4'a), 83.5(C1'a), 81.4 (d, $J = 8.2$ Hz, C3'a), 70.7 (C3'b), 68.0 (d, $J = 3.7$ Hz, C5'b), 58.4 (C5'a), 55.2 (OMe), 49.1 (C2'a), 39.9 (C2'b), 37.7 (C7'a), 13.4 (7'-Me), 12.5 (T-Me), 11.9 (T-Me). MALDI-TOF M/S: $[M + Na]^+$ found 909.305, calcd 909.2725. **16b**. ^{31}P NMR (202.5 MHz, $CDCl_3$): δ -5.0. 1H NMR (500 MHz, $CDCl_3$): δ 7.78 (s, 1H, H6), 7.41-6.83 (m, 14H), 6.22 (dd, $J_{H1'b,H2'b} = 6.4$ Hz, $J_{H1'b,H2''b} = 5.5$ Hz, 1H, H1'b), 5.63 (s, 1H, H1'a), 5.10 (d, $J_{H3'a,p} = 17.4$ Hz, 1H, H3'a), 4.24 (m, 1H, H3'b), 4.13 (ddd, $J_{H5'b,H4'b} = 5.4$ Hz, $J_{H5'b,H5''b} = J_{H5'b,p} = 11.9$ Hz, 1H, H5'b),

4.10 (ddd, $J_{H5'b,H4'b} = 2.7$ Hz, $J_{H5'b,H5''b} = J_{H5'b,p} = 11.9$ Hz, 1H, H5''b), 4.01 (d, $J_{H6'a,p} = 24.6$ Hz, 1H, H6'a), 3.91 (d, $J_{H5'a,H5''a} = 11.3$ Hz, 1H, H5'a), 3.86 (d, $J_{H5'a,H5''a} = 11.3$ Hz, 1H, H5''a), 3.78-3.79 (m, 7H, H4'b, OMe), 3.27 (m, 2H, H2'a, H7'a), 2.37 (m, 1H, H2'b), 2.06 (m, 1H, H2''b), 1.74 (s, 3H, T-Me), 1.43 (d, $J_{H7'a,7'Me} = 6.4$ Hz, 3H, 7'-Me), 1.25(s, 3H, T-Me). ^{13}C NMR (125 MHz, $CDCl_3$): δ 163.9(C4), 163.6 (C4), 158.9, 158.8, 150.1 (C2), 149.8 (C2), 143.9, 135.5, 134.8, 134.7, 134.5, 130.4, 130.3, 128.1, 128.0, 127.5, 113.5, 113.4, 110.8 (C5), 87.3, 84.5 (C1'b), 84.2 (d, $J = 2.2$ Hz, C4'b), 84.0 (d, $J = 4.9$ Hz, C6'a), 83.4 (C1'a), 83.3 (d, $J = 6.9$ Hz, C4'a), 81.0 (d, $J = 9.7$ Hz, C3'a), 69.6 (C3'b), 67.4 (d, $J = 6.2$ Hz, C5'b), 58.7 (C5'a), 55.3 (OMe), 49.4 (C2'a), 39.6 (C2'b), 39.3 (C7'a), 13.4 (7'-Me), 12.3 (T-Me), 11.7 (T-Me). MALDI-TOF M/S: $[M + Na]^+$ found 909.345, calcd 909.2725.

(S_p)-D₂-CNA-dT (17a). **16a** (20 mg) was dissolved in 2 mL of 2% TFA in CH_2Cl_2 and stirred at room temperature for 3 min. Ten milliliters of double-distilled water was added to the reaction mixture and the organic phase was removed. The aqueous phase was washed with CH_2Cl_2 twice. The crude product in the aqueous phase was purified by RP-HPLC (Kromasil 100, C18, 5 μ m, 250 \times 8 mm. 0-40', C- \rightarrow C/D = 60/40, v/v; flow rate 1.5 mL/min at room temperature; Buffer C: 5% MeOH in H₂O; Buffer D: pure MeCN) to give **17a** (10 mg, $t_R = 28.8$ min). **17a**. ^{31}P NMR (202.5 MHz, D₂O): δ -6.4. 1H NMR (500 MHz, D₂O): δ 7.78 (s, 1H, H6), 7.75 (s, 1H, H6), 6.23 (dd, $J_{H1'b,H2'b} = 6.4$ Hz, $J_{H1'b,H2''b} = 7.0$ Hz, 1H, H1'b), 5.61 (s, 1H, H1'a), 4.89 (d, $J_{H3'a,p} = 17.0$ Hz, 1H, H3'a), 4.44 (m, 1H, H3'b), 4.36 (ddd, $J_{H5'b,H4'b} = 2.7$ Hz, $J_{H5'b,p} = 6.5$ Hz, $J_{H5'b,H5''b} = 11.6$ Hz, 1H, H5'b), 4.31-4.25 (m, 2H, H5''b, H6'a), 4.24 (d, $J_{gem} = 14.0$ Hz, 1H, H5'a), 4.18 (d, $J_{gem} = 14.0$ Hz, 1H, H5''a), 4.13 (m, 1H, H4'b), 3.03 (d, $J_{H2'a,H7'a} = 4.9$ Hz, 1H, H2'a), 2.95 (m, 1H, H7'a), 2.40-2.28 (m, 2H, H2'b, H2''b), 1.82 (s, 3H, T-Me), 1.79 (s, 3H, T-Me), 1.24 (d, $J_{H7'a,7'Me} = 7.4$ Hz, 3H, 7'-Me). ^{13}C NMR (125 MHz, D₂O): δ 166.6, 166.3(C4), 151.6, 150.8 (C2), 137.4, 136.5, 110.3, 110.4 (C5), 85.5 (C1'b), 84.5 (d, $J = 6.9$ Hz, C6'a), 84.1 (d, $J = 6.9$ Hz, C4'b), 84.0(d, $J = 6.9$ Hz, C4'a), 83.5(C1'a), 81.6 (d, $J = 8.3$ Hz, C3'a), 70.1 (C3'b), 68.1 (d, $J = 5.5$ Hz, C5'b), 56.4 (C5'a), 48.6 (C2'a), 38.2 (C2'b), 37.6 (C7'a), 12.3 (7'-Me), 11.7 (T-Me), 11.5 (T-Me). MALDI-TOF M/S: $[M + Na]^+$ found 607.070, calcd 607.1417.

(S_p)-D₂-CNA-dT (17b). **16b** (17 mg) was dissolved in 2 mL of 2% TFA in CH_2Cl_2 and stirred at room temperature for 3 min. Ten milliliters of double distilled water was added to the reaction mixture, and the organic phase was removed. The aqueous phase was washed with CH_2Cl_2 twice. The crude product in the aqueous phase was purified by RP-HPLC (Kromasil 100, C18, 5 μ m, 250 \times 8 mm. 0-40', C- \rightarrow C/D = 60/40, v/v; flow rate 1.5 mL/min at room temperature; Buffer C: 5% MeOH in H₂O; Buffer D: pure MeCN) to give **17b** (10 mg, $t_R = 29.07$ min). **17b**. ^{31}P NMR (202.5 MHz, D₂O): δ -4.6. 1H NMR (500 MHz, D₂O): δ 7.81 (s, 1H, H6), 7.44 (s, 1H, H6), 6.20 (dd, $J_{H1'b,H2'b} = 6.7$ Hz, $J_{H1'b,H2''b} = 6.4$ Hz, 1H, H1'b), 5.63 (s, 1H, H1'a), 4.09 (d, $J_{H3'a,p} = 16.1$ Hz, 1H, H3'a), 4.47 (m, 1H, H3'b), 4.39-4.27 (m, 2H, H5'b, H5''b), 4.23 (d, 1H, $J_{H5'b,p} = 25.2$ Hz, H6'a), 4.15 (d, $J_{gem} = 13.9$ Hz, 1H, H5'a), 4.08 (m, 2H, H5''a, H4'b), 3.21 (d, $J_{H2'a,H7'a} = 4.7$ Hz, 1H, H2'a), 2.92 (m, 1H, H7'a), 2.37-2.34 (m, 2H, H2'b, H2''b), 1.82 (s, 3H, T-Me), 1.81 (s, 3H, T-Me), 1.31 (d, $J_{H7'a,7'Me} = 7.3$ Hz, 3H, 7'-Me). ^{13}C NMR (125 MHz, D₂O): δ 166.6, 166.4 (C4), 151.7, 151.0 (C2), 137.3, 136.6, 111.2, 110.4 (C5), 85.4 (C1'b), 84.2 (d, $J = 6.1$ Hz, C6'a), 83.9 (d, $J = 6.9$ Hz, C4'b), 83.8 (d, $J = 6.9$ Hz, C4'a), 83.2(C1'a), 81.4 (d, $J = 9.4$ Hz, C3'a), 69.7 (C3'b), 67.8 (d, $J = 5.4$ Hz, C5'b), 56.5 (C5'a), 48.7 (C2'a), 39.7 (C2'b), 37.9 (C7'a), 12.3 (7'-Me), 11.7 (T-Me), 11.5 (T-Me). MALDI-TOF M/S: $[M + H]^+$ found 585.105, calcd 585.1598.

3'b-(2-(Cianoethoxy(diisopropylamino)phosphinoxy))-5'a-(4,4'-dimethoxytrityloxymethyl)- (S_p)-D₂-CNA-dT (18). Compound **17a** (75 mg, 0.085 mmol) was dissolved in dry THF (3 mL), and DIPEA (0.057 mL, 0.34 mmol) was added. The mixture was cooled with ice, and 2-cyanoethyl-*N,N*-diisopropylphosphoramidochloridite (0.037 mL, 0.17 mmol) was added dropwise to the

solution under N₂. After being stirred for 1 h at rt, the reaction was quenched with methanol and stirred further 10 min. Then the reaction mixture was diluted with ethyl acetate and washed with saturated NaHCO₃ solution, dried over MgSO₄, and subjected to chromatography on silica gel (ethyl acetate in CH₂Cl₂ containing 1% Et₃N, 50–70%, v/v) to give **18** (64 mg, 70%). ³¹P NMR (202.5 MHz, CDCl₃): δ 149.4, 149.3, –8.12, –8.15. MALDI-TOF M/S: [MH]⁺ found 1087.18, calcd 1087.40.

Carba-LNA-6',5'-dT (21), Carba-LNA-3',5'-dT (22), and Carba-LNA-6',3'-dT (23). Dimer **17a** (10 mg) was treated with 5 mL of 0.3 M NaOH for 24 h and then quenched with 5 mL of 0.3 M AcOH. The crude product was purified by RP-HPLC (Kromasil 100, C18, 5 μ, 100 × 4.6 mm. 0→10'→20', A→A/B = 1/9 → A/B = 62/38, v/v. Flow of 1 mL/min was used at room temperature using a UV detector with detecting wavelength of 260 nm) to give products **21** (t_R = 10.19 min), **22** (t_R = 11.49 min) and **23** (t_R = 12.82 min). **21**. ³¹P NMR (202.5 MHz, D₂O): δ –0.92. ¹H NMR (500 MHz, D₂O): δ 7.68 (s, 1H, H6), 7.61 (s, 1H, H6), 6.25 (dd, J = 6.5 Hz, J = 7.0 Hz, 1H, H1'b), 5.50 (s, 1H, H1'a), 4.52 (m, 1H, H3'b), 4.42 (s, 1H, H3'a), 4.07 (m, 1H, H' b), 4.04–3.92 (m, 4H, H5'b, H5''b, H5'a, H5''a), 3.77 (ddd, J_{H6'b,H7'a} = 3.7 Hz, J_{H6'a,p} = 8.9 Hz, ^wJ_{H6'a,H3'a} = 1.5 Hz, 1H, H6'a), 2.62 (m, 1H, H7'a), 2.54 (d, J_{H2'a,H7'a} = 3.9 Hz, 1H, H2'a), 2.37–2.31 (m, 2H, H2'b, H2''b), 1.85 (s, 3H, T-Me), 1.82 (s, 3H, T-Me), 1.24 (d, J_{H7'a,7'Me} = 7.4 Hz, 3H, 7'-Me). ¹³C NMR (125 MHz, D₂O): δ 166.9, 166.8(C4), 152.1, 151.4 (C2), 137.6, 137.2, 111.5, 109.9 (C5), 88.6 (d, J = 6.9 Hz, C4'a), 85.1 (C1'b), 85.1 (d, J = 8.3 Hz, C4'b), 83.4(C1'a), 82.0 (d, J = 6.2 Hz, C6'a), 71.6 (C3'a), 70.5 (C3'b), 65.1 (d, J = 5.5 Hz, C5'b), 56.9 (C5'a), 49.5 (C2'a), 39.2 (d, J = 1.4 Hz, C7'a), 38.3(C2'b), 12.5 (7'-Me), 11.8 (T-Me), 11.7 (T-Me). MALDI-TOF M/S: [M+H]⁺ found 603.041, calcd 603.1704. **22**. MALDI-TOF M/S: [M + Na]⁺ found 625.105, calcd 625.1523. The standard sample **22** has been synthesized using 6'-R-OTol-7'-S-methylcarba-LNA phosphoramidite,³⁰ and here coinjection of product **22** with standard sample showed they were identical. **23**. ³¹P NMR (202.5 MHz, D₂O): δ –1.30. ¹H NMR (500 MHz, D₂O): δ 7.69 (s, 1H, H6), 7.59 (s, 1H, H6), 6.27 (dd, J = 7.5 Hz, J = 6.2 Hz, 1H, H1'b), 5.62 (s, 1H, H1'a), 4.75 (1H, H3'b, merged in solvent peak), 4.18 (m, 2H, H3'a, H4'b), 3.40 (d, J_{gem} = 13.2 Hz, 1H, H5'a), 3.97 (d, J_{gem} = 13.2 Hz, 1H, H5''a), 3.85 (ddd, J_{H6'b,H7'a} = 3.4 Hz, J_{H6'a,p} = 8.9 Hz, ^wJ_{H6'a,H3'a} = 1.4 Hz, 1H, H6'a), 3.78 (dd, J_{gem} = 12.5 Hz, J_{H4'b,H5'a} = 3.5 Hz, 1H, H5'b), 3.72 (dd, J_{gem} = 12.5 Hz, J_{H4'b,H5'a} = 5.0 Hz, 1H, H5''b), 2.67 (m, 1H, H7'a), 2.61 (dd, J_{H2'a,H7'a} = 4.1 Hz, J_{H2'a,H3'a} = 1.3 Hz, 1H, H2'a), 2.51 (ddd, J_{H2'b,H1'b} = 6.2 Hz, J_{H2'b,H3'b} = 2.8 Hz, J_{H2'b,H2''b} = 14.3 Hz, 1H, H2'b), 2.35 (m, 1H, H2''b), 1.84 (s, 6H, T-Me), 1.31 (d, J_{H7'a,7'Me} = 7.4 Hz, 3H, 7'-Me). ¹³C NMR (150 MHz, D₂O): δ 166.7(C4), 152.1, 152.0 (C2), 137.3, 137.1, 111.6, 109.9 (C5), 88.6(d, J = 6.9 Hz, C4'a), 84.1 (d, J = 6.9 Hz, C4'b), 85.1 (C1'b), 83.4(C1'a), 82.1 (d, J = 6.9 Hz, C6'a), 75.3 (d, J = 2.8 Hz, C3'b), 71.7 (C3'a), 61.2 (C5'b), 57.1 (C5'a), 49.5 (C2'a), 39.0 (C7'a), 37.6 (C2'b), 12.5 (7'-Me), 11.9 (T-Me), 11.6 (T-Me). MALDI-TOF M/S: [M + Na]⁺ found 603.071, calcd 603.1704.

Theoretical Calculations. The geometry optimizations of the (D₂-CNA dT)-dT **17a** and **17b** have been carried out by GAUSS-IAN 98 program package⁴⁰ at the Hartree–Fock level using 6-31G**. Relevant vicinal proton ³J_{HH} coupling constants have been back-calculated from the corresponding theoretical torsions employing Haasnoot–de Leeuw–Altona-generalized Karplus equation^{38,39} taking into account β substituent correction in the form

$${}^3J = P_1 \cos^2(\phi) + P_2 \cos(\phi) + P_3 + \sum(\Delta\chi_i^{\text{group}}(P_4 + P_5 \cos^2(\xi_i \phi + P_6 |\Delta\chi_i^{\text{group}}|)))$$

where $\Delta\chi_i^{\text{group}} = \Delta\chi_i^{\alpha\text{-substituent}} - P_7 \sum \Delta\chi_i^{\beta\text{-substituent}}$ and $\Delta\chi_i$ are taken as Huggins electronegativities.⁷⁵ $P_1 = 13.70$, $P_2 = -0.73$,

$P_3 = 0.00$, $P_4 = 0.56$, $P_5 = -2.47$, $P_6 = 16.90$, $P_7 = 0.14$ (parameters from reference³⁸).

The simplified Karplus equation has been used to calculate the proton-phosphorus and carbon–phosphorus vicinal coupling constants ³J_{CCOP} (³J_{POCH}) = A cos²(φ) + B cos(φ) + C, where the Karplus (A, B, C) parameters are A = 9.1, B = –1.9, C = 0.8 for the ³J_{CCOP} coupling constants and A = 15.3; B = –6.2; C = 1.5 for the ³J_{POCH} as in ref 48.

Stability of Dimer Nucleotides in 1 mM NaOH Solution. To the lyophilized solid dimers (1 OD at A_{260nm}) in an Eppendorf tube was added 1 mL of aqueous sodium hydroxide (1mM). The mixture was allowed to stand at 21 °C, and aliquots (100 μL) were taken at regular intervals, and immediately quenched with 100 μL of aqueous acetic acid (1 mM) to ca. pH 7. Then the aliquots were analyzed by RP-HPLC. The total percentage of intact dimers was plotted against time points to give the degradation curves, and the pseudo-first-order reaction rates were obtained by fitting the curves to single-exponential decay functions.

Stability of D₂-CNA-dT Dimers in Concentrated Ammonia Solution. To the lyophilized solid dimer (S_p)-D₂-CNA dT dimer **17a** or (R_p)-D₂-CNA dT dimer **17b** (0.1 OD at A_{260nm}) in an Eppendorf tube, 100 μL of 33% aqueous ammonium solution was added. The mixture was allowed to stand at 21 °C. The reaction was quenched with 100 μL of acetic acid at the end of the reaction and analyzed by RP-HPLC. The total percentage of intact dimers was plotted against different time points to give the degradation curves, and the pseudo-first-order reaction rates were obtained by fitting the curves to single-exponential decay functions.

Stability of D₂-CNA-dT Dimers in Hydrazine Hydrate. To the lyophilized solid (S_p)-D₂-CNA dT dimer **17a** or (R_p)-D₂-CNA dT dimer **17b** (1 OD at A_{260nm}) in an Eppendorf tube was added 0.5 mL of 0.5 M hydrazine hydrate in pyridine/AcOH (4/1, v/v). The mixture was allowed to stand at 21 °C, and aliquots (50 μL) were taken at regular intervals, immediately diluted with 350 μL of H₂O, and lyophilized. Then the aliquots were analyzed by RP-HPLC. The total percentage of integrated dimers was plotted against time points to give the degradation curves, and the pseudo-first-order reaction rates were obtained by fitting the curves to single-exponential decay functions.

Stability of D₂-CNA-dT Dimers in DBU. To the lyophilized solid (S_p)-D₂-CNA dT dimer **17a** or (R_p)-D₂-CNA dT dimer **17b** (1 O. D. at A_{260 nm}) in an Eppendorf tube was added 0.5 mL of 0.5 M DBU in dry MeCN. The mixture was allowed to stand at 21 °C, and aliquots (50 μL) were taken at regular intervals, immediately diluted with 350 μL of 1 M TEAA, and lyophilized. Then the aliquots were analyzed by RP-HPLC. The total percentage of integrated dimers was plotted against time points to give the degradation curves, and the pseudo-first-order reaction rates were obtained by fitting the curves to single-exponential decay functions.

SVPDE Degradation Studies. One OD (A_{260nm}) dimer was incubated in 1 mL of buffer (100 mM Tris–HCl (pH 8.0) and 15 mM MgCl₂) with 3 μg/mL of phosphodiesterase I from *Crotalus adamanteus* (SVPDE, obtained from USB Corp., Cleveland, OH) at 21 °C. Aliquots (100 μL) were taken at regular intervals and quenched with 100 μL of 10 mM EDTA solution followed by freezing with anhydrous ice quickly. Then the aliquots were analyzed by RP-HPLC. The total percentage of integrated dimers was plotted against time points to give the degradation curves, and the pseudo-first-order reaction rates could be obtained by fitting the curves to single-exponential decay functions.

Oligonucleotide Synthesis, Deprotection, and Purification. AONs 2–5 were synthesized using an automated DNA/RNA synthesizer based on phosphoramidite chemistry. Ac-dC SyBase CPG 1000/110 solid support was obtained from Link Technologies (UK). For native A and C building blocks, fast deprotecting phosphoramidites (Ac for C, Pac for A) were used. Standard DNA synthesis reagents and cycles were used except that 0.25 M 5-ethylthio-1H-tetrazole was used as the activator, 0.02 M iodine as the oxidizer, and Tac₂O as the cap A. After synthesis, solid

(75) Huggins, M. L. *J. Am. Chem. Soc.* **1953**, *75*, 4123–4126.

supports (0.2 μmol scale) in Eppendorf tubes were incubated with 1 mL of dry $\text{Et}_3\text{N}/\text{MeCN}$ (3/2, v/v) at room temperature for 1 h. The supernatant was decanted, another 1 mL of dry $\text{Et}_3\text{N}/\text{MeCN}$ (3/2, v/v) was added, and the mixture was kept at room temperature for another 1 h. The supernatant was removed again, and the solid support was dried in air and then treated with 1 mL of 0.5 M DBU in dry MeCN at room temperature. After 24 h, the reaction was quenched with 30 μL of acetic acid. The supernatant was moved to another Eppendorf tube and lyophilized. The obtained residue was then incubated with 1 mL of 0.5 M hydrazine hydrate in pyridine/AcOH (4/1, v/v) at room temperature for 24 h and lyophilized. The obtained residue was applied to NAP-10 column (GE Healthcare, Sweden) to give crude product which was purified by HPLC to give pure AON. The correct masses have been obtained by MALDI-TOF mass spectroscopy for all AONs **2–5** (Table 2).

The pure AONs **6–9** were obtained according to our previous report.³⁰ The AONs **10–13** were obtained by the following procedure: The solid supports of AONs **2–5** was incubated with 33% aqueous ammonia for 4 h at room temperature. Evaporation of the solvent on vacuum gave the crude products. These crude products were supposed to contain two components: treatment of AON **2** with ammonia gave AON **10** as the major product plus small amount of AON **6**; AON **3** gave AON **11** (major) plus AON **7** (minor), AON **4** gave AON **12** (major) plus AON **8** (minor), and AON **5** gave AON **13** (major) plus minor AON **9** (minor). AON **11** (83%) can be separated from AON **7** (17%) by RP-HPLC and so was obtained in pure form, whereas AON **10** cannot be separated from AON **6**, AON **12** cannot be separated from AON **8**, AON **13** cannot be separated from AON **9**, and so AON **10**, **12**, and **13** were only obtained in about 80% purity.

UV Melting Experiments. Determination of the T_m of the AON/RNA hybrids or AON/DNA duplex was carried out in the following buffer: 60 mM Tris-HCl (pH 7.5), 60 mM KCl, 0.8 mM MgCl_2 .

Absorbance was monitored at 260 nm in the temperature range from 18 to 60 $^\circ\text{C}$ using an UV spectrophotometer equipped with a Peltier temperature programmer with the heating rate of 1 $^\circ\text{C}$ per minute. Prior to measurements, the samples (1 μM of AON and 1 μM cDNA or RNA mixture) were preannealed by heating to 80 $^\circ\text{C}$ for 5 min followed by slow cooling to 15 $^\circ\text{C}$ and 30 min equilibration at this temperature. The value of T_m is the average of two or three independent measurements.

CD Experiments. CD spectra were recorded from 300 to 220 nm in 0.2 cm path length cuvettes. Spectra were obtained with concentration of 0.1 mM dimers in 60 mM Tris-HCl (pH 7.5), 60 mM KCl, 0.8 mM MgCl_2 . All of the spectra were measured at 5 $^\circ\text{C}$.

Acknowledgment. Generous financial support from the Swedish Natural Science Research Council (Vetenskapsrådet), the Swedish Foundation for Strategic Research (Stiftelsen för Strategisk Forskning), and the EU-FP6 funded RIGHT project (Project no. LSHB-CT-2004-005276) is gratefully acknowledged. We thank Dr. N. Badgajar for providing starting material **1** for this study.

Supporting Information Available: ^1H , ^{13}C , COSY, HMQC, HMBC, DEPT, and NOESY NMR spectra of compounds **2–23**. Input information of ab initio geometry optimizations in GAUSSIAN 98 program for compounds **17a** and **17b**. Atom coordinates and absolute energies of optimized structure of compounds **17a** and **17b**. RP-HPLC profiles: mass spectra of oligo AONs **2–13**. Melting curves of AON/DNA and AON/RNA duplexes. This material is available free of charge via the Internet at <http://pubs.acs.org>.

JO900391N